Airflow Configurations of Warm Season Southerly Low-Level Wind Maxima in the Great Plains. Part II: The Synoptic and Subsynoptic-Scale Environment

CLAUDIA K. WALTERS

Department of Geography, Central Michigan University, Mount Pleasant, Michigan

(Manuscript received 24 May 2000, in final form 9 May 2001)

ABSTRACT

Twelve different spatial configurations of southerly warm season low-level wind maxima in the Great Plains were identified in Part I, based on streamline orientation and curvature, the location of confluence and deformation zones, and the latitudinal extent of the wind maxima. Here, in Part II, composite analysis was employed to examine the typical lower, mid-, and upper-tropospheric environments for the 12 configuration types. Only two of the jet types were found to occur in association with a midtropospheric ridge, an environment that has previously been labeled as quiescent. These two jet types had a fairly simple anticyclonic airflow configuration. The remaining 10 configuration types occurred in association with a trough over the southwestern United States and a ridge to the east (i.e., an active environment). Consequently, the pronounced differences in the airflow configuration identified in this study are associated with an active midtropospheric pattern.

Only 1 of the 12 configuration types appeared to be a purely boundary layer-driven wind maximum. For the remaining types, the relative influence of synoptic forcing and boundary layer forcing varied, as inferred from the relative strength of the geostrophic and ageostrophic wind components and the climatological characteristics of the wind maxima (e.g., average elevation and the typical time of day and month of occurrence). The location of the jet core for all configuration types reflected a combination of the geostrophic and ageostrophic contributions to the actual wind. Areas of large ageostrophic wind vectors were generally located to the west/northwest and to the south of the jet core, and are thought to represent transverse circulations around a confluence/frontal zone and around a dryline, respectively. The ageostrophic wind vectors also displayed a veering (i.e., anticyclonic rotation) upstream of the jet core. For most jet types, the right entrance quadrant of a 200-mb jet streak was positioned over the low-level wind maximum.

The results of Part I and Part II, taken together, illustrate the considerable variability both in the physical characteristics of warm season low-level wind maxima in the Great Plains and in the large-scale environment in which these wind maxima occur. This variability must be kept in mind when forecasting convection in association with low-level wind maxima, and when interpreting previous case studies of low-level wind maxima or earlier climatological studies based on a small number of events.

1. Introduction

This paper is the second part of a two-part study that addresses the variations in the airflow configurations of low-level wind maxima in the Great Plains and the synoptic and subsynoptic-scale environments in which the wind maxima form. In Part I (Walters and Winkler 2001) 12 distinct airflow configurations for low-level wind maxima were identified using a subjective typing scheme that considered streamline curvature, location and orientation of confluence and deformation zones, and latitudinal extent of southerly jet events that occurred during the 1991 and 1992 warm seasons. The configuration types included anticyclonically curved low-level wind maxima, bifurcating wind maxima with cyclonically and anticyclonically turning arms, cyclonically curved maxima, and complex types that displayed a closed cyclonic circulation. For several of the types, either a convergence zone or a deformation zone was evident downstream of the isotach maximum. In addition, a southwest–northeast-oriented confluence zone was present along the west (left) flank of the wind maximum for almost all jet types. Six of the 12 types had relatively small latitudinal extents of approximately 10°–15° latitude, whereas the other 6 had latitudinal extents of approximately 15°–25° latitude. Over 50% of the jet events were considered ''complex'' in that the airflow configuration changed in the vertical, in general becoming more anticyclonically curved with height. These ''multiple airstreams'' resulted in several areas of convergence that were displaced horizontally with respect to one another. The location of these multiple convergence zones was often mirrored in the spatial distribution of cloud-to-ground lightning flashes. The most frequent lightning activity generally was collocated with areas of strong convergence.

Corresponding author address: Claudia K. Walters, Department of Geography, Central Michigan University, Dow 296A, Mount Pleasant, MI 48859.
E-mail: walters234@earthlink.net

It is reasonable to assume that, given the varying spatial patterns and other characteristics of the identified jet types, the environment in which the jet types form also varies. The aim of this paper (i.e., Part II) is to investigate variations in the synoptic and subsynoptic-scale environment of the different jet types. In the following section, previously identified physical mechanisms that lead to the formation and intensification of low-level wind maxima are briefly reviewed. In section 3, the data that were used in this study and the analysis methods are introduced. The typical environments of the 12 different airflow configuration types are described in section 4, and in section 5 they are discussed in relation to previous research. The major findings of Part I and Part II are summarized in section 6.

2. Background

Low-level wind maxima have been observed in a variety of synoptic settings. Increasingly, investigators are calling for a distinction to be made between spatially extensive wind maxima that appear to be related to synoptic-scale forcing and more localized wind maxima that are primarily controlled by boundary layer or lower-tropospheric forcing (e.g., Uccellini 1980; Chen et al. 1994; Stensrud 1996). For example, Uccellini (1980) and Igau and Nielsen-Gammon (1998) differentiate between two broad types of Great Plains low-level wind maxima. The first type is associated with a trough upstream and a ridge downstream of the southern Great Plains and with an upper-tropospheric jet streak propagating into the region. This environment has been termed active by Igau and Nielsen-Gammon (1998). The second type forms in a quiescent environment dominated by a midtropospheric ridge (Igau and Nielsen-Gammon 1998). In this setting, wind maxima typically form under conditions of 1) an east-to-west sea level pressure gradient resulting from a large-scale anticyclone to the east and a warm low pressure area to the west, 2) cloudless nights, 3) strong afternoon insolation, and 4) no intruding fronts (Hoecker 1965). However, the physical mechanisms leading to the development and enhancement of low-level wind maxima that form in active environments and those that form in quiescent environments are not mutually exclusive. Rather, Djuric and Ladwig (1983) and Mitchell et al. (1995) point out that synoptically driven wind maxima are often enhanced by favorable boundary layer conditions.

A number of physical mechanisms have been put forth to explain the occurrence and development of low-level wind maxima (see Stensrud 1996 for a more complete discussion). Boundary layer influences include differential heating over the sloping terrain of the Great Plains and Rocky Mountains (Bonner and Paegle 1970; Fast and McCorcle 1990), diurnal changes in eddy viscosity (Blackadar 1957; Buajitti and Blackadar 1957; Bonner and Paegle 1970; Paegle and Rasch 1973), and frictional decoupling (Hoecker 1965; Hoxit 1975; Parish et al. 1988). The rapid change of the nocturnal boundary layer from a convective regime in the afternoon hours to a stable regime at night was seen by Zeman (1979) as a prerequisite for generating large geostrophic departures that ultimately make possible a supergeostrophic wind maximum during the nighttime and early morning (Blackadar 1957). The resulting low-level wind maximum is frequently observed at the top of the nocturnal inversion (Blackadar 1957; Izumi 1964). Jets have been shown to persist into the daytime hours when overcast cloudiness reduces insolation enough to suppress the turbulent stress needed to dissipate the jet (Hoecker 1963). The diurnal oscillation in height and speed of the boundary layer jet is typically accompanied by a clockwise rotation of wind direction with time (Blackadar 1957; Hering and Borden 1962; Hoecker 1965; Hoxit 1975). This rotation is attributed to an inertial component of period 12 pendulum hours that is imposed on the actual wind at the time of the release of surface friction (Blackadar 1957; Wexler 1961; Hoecker 1963).

Parish et al. (1988) showed that the ageostrophic portion of low-level wind maxima is composed of both an isallobaric component and an inertial-advective component. For low-level wind maxima that are primarily boundary-layer features, the isallobaric flow is believed to be induced by a relaxing of an east–west pressure gradient and the subsequent decrease in the southerly geostrophic wind. In this situation, the isallobaric component generally is secondary in importance to the inertial-advective component caused by frictional decoupling (Parish et al. 1988). For synoptically driven low-level jets, the isallobaric wind component is associated with large-scale surface pressure falls that occur in conjunction with cyclogenesis and/or a propagating upper-level jet streak (Uccellini 1980; Djuric 1981; Djuric and Ladwig 1983).

Upper-tropospheric wind fields also play a role in the formation of low-level jets. Achtor and Horn (1986) found that the strength of low-level wind maxima within developing cyclones is directly related to the strength of the upper-tropospheric wind field. A number of authors have shown that an upper-tropospheric divergent center located in the exit region of an upper-level jet streak, and ahead of an upper-level trough, is matched by a lower-tropospheric convergent center (Sechrist and Whittaker 1979; Uccellini and Johnson 1979; Achter and Horn 1986; Chen and Kpaeyeh 1993). A low-level jet is then accelerated by the isallobaric wind component toward the lower-tropospheric low pressure center (Sjostedt et al. 1990; Uccellini 1990; Chen and Kpaeyeh 1993). This jet has a generally south-to-north orientation and is directed toward the left exit (front) quadrant of the upper-level wind maximum (Uccellini and Johnson 1979; Achter and Horn 1986).

Finally, southerly low-level wind maxima have been observed embedded within the ''warm conveyor belt'' of midlatitude cyclones. These wind maxima typically

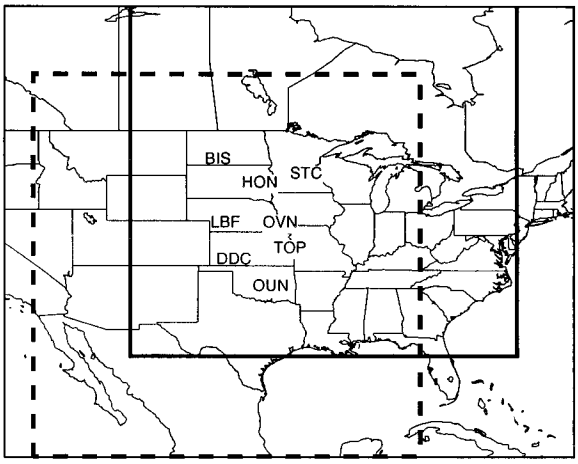

FIG. 1. Eight rawinsonde stations in the central United States that were used to identify vertical jet profile signatures. Analysis of the lower-, mid-, and upper-tropospheric variables employed all rawinsonde stations across the larger area. The two smaller boxes (bold and dashed) illustrate the size of the subgrid used to prepare the composite analyses.

are aligned along the comma ''tail'' of the low pressure system (Carr and Millard 1985) and are located close to a surface cold frontal boundary (Browning and Pardoe 1973). Kotroni et al. (1994) attribute the formation of a low-level wind maximum within the warm conveyor belt to a locally strong horizontal temperature gradient. They speculate that this temperature gradient is intensified by ageostrophic circulations that are part of a thermally direct cross-frontal circulation. A secondary circulation around the low-level jet axis, with strong ascending motion on the left flank of the jet and weaker subsidence on the right flank, has also been observed (Browning and Pardoe 1973; Kotroni et al. 1994).

3. Data and methods

The data and methods used to identify the jet events for this study are described in detail in Part I. Briefly, jet events for two warm seasons (Apr–Sep 1991 and 1992) were identified and classified using the following procedures. First, vertical wind profiles were plotted for eight rawinsonde stations in the Great Plains (Fig. 1), and those profiles that displayed a speed maximum, referred to as a jet profile signature, were retained for further analysis. Second, streamlines and isotach fields were plotted for the constant pressure surface at the elevation of the strongest wind speed within each of the jet profile signatures. Rawinsonde observations for all stations that fell within the area bounded by 20°–60°N and 70°–120°W were used to create these plots. Third, the multiple plots per observation time were collapsed into one ''jet event.'' Jet events have both horizontal and vertical dimensions, and multiple jet profile signatures can be part of the same jet event. The jet events were considered to be ''simple'' or ''complex,'' depending on whether the airflow configuration on the multiple pressure surfaces changed with height. To account for the differences in height, up to three analysis levels were chosen. Note that all analysis levels were located below and up to 700 mb. Fourth, the airflow configuration for the lowest analysis level (i.e., the one closest to the surface) was used to subjectively type the jet events based on 1) their latitudinal extent, 2) the degree and orientation of streamline curvature, and 3) the existence and orientation of confluence, diffluence, and deformation zones. Only those jet events with at least one streamline originating over the Gulf of Mexico were included in the typing procedure. A total of 260 jet events were classified into 12 different airflow configuration types with 10 or more events.

A compositing approach was used to characterize the typical synoptic and subsynoptic-scale environment for each of the 12 jet configuration types. Average fields were computed for several lower-, mid-, and upper-tropospheric parameters including 500-mb geopotential height, 200-mb u and v wind components, 200-mb divergence, sea level pressure, and 12-h sea level pressure tendency. In addition, composite geostrophic and ageostrophic wind fields for the lowest analysis level were computed. Only the total ageostrophic wind field was considered, as it was not possible in this study to distinguish between the inertial-advective and isallobaric components. The composite fields were computed by first interpolating the observed values for each parameter and jet event to a 1° latitude by 1° longitude grid using the Barnes method (Koch et al. 1983). Next, a subgrid with dimensions of 35° latitude by 35° longitude was extracted from the interpolated fields. The subgrid had the same grid spacing as the larger grid and was positioned on the approximate center of the isotach maximum for each jet event. The subgrids were then averaged across all events for each configuration type, and the mean fields were plotted.

Composite analysis provides an objective method for identifying key features from multiple cases, in that, ideally, it emphasizes commonly occurring features while smoothing more random fluctuations. However, due to case-to-case variability, the average fields tend to be weaker than what would be observed for an individual case. Readers should bear this in mind when interpreting the composite analyses presented here.

4. Synoptic and subsynoptic-scale environments of low-level wind maxima

The following section describes the composite lower-, mid-, and upper-level environments of the 12 airflow configuration types. The six jet types with smaller latitudinal extent (approximately 10°–15° of latitude) are described first, followed by the six types with larger (15°–25°) latitudinal extent. The acronyms used to describe the individual jet types are defined in Table 1. Key features

TABLE 1. Acronyms used to denote jet types.

A	Anticyclonically curved	c	Confluence zone
B	Bifurcating flow	d	Deformation zone
C	Cyclonically curved	EW	East–west
K	Kurl*	SWNE	Southwest–northeast
L	Long	NWSE	Northwest–southeast

* The term kurl is used instead of closed cyclonic circulation to facilitate a distinction in the acronyms used for the different types. The letter C already stands for cyclonically curved in the notation employed.

of the synoptic and subsynoptic-scale environments for each jet type are summarized in Table 2.

a. Anticyclonically curved jet with confluence zone oriented east–west (Ac-EW jets)

The composite 500 mb-geopotential height field indicates that Ac-EW jets typically occur near the axis of a weak midtropospheric ridge located over the southern portion of the analysis region (Fig. 2). This pattern suggests that Ac-EW jets form in a quiescent environment. However, some features that would be expected in an active environment are also present. For example, a fairly strong 500-mb height gradient is evident immediately north of the jet core. This gradient supports relatively strong upper-level winds, as seen from the 200-mb composite wind field. Ac-EW jets are typically located beneath the right entrance quadrant of an upper-level jet streak, theoretically an area of upper-level divergence. The mean 200-mb divergence field displays a local maximum of divergence immediately downstream of the low-level jet core.

The composite sea level pressure field for Ac-EW jets resembles a col. A low pressure system to the northeast of the wind maximum and a high pressure system to the northwest are evident. These surface features likely contribute to the limited latitudinal extent of Ac-EW jets. The col is completed by a second cyclone in the southwestern portion of the analysis region and a second anticyclone to the southeast. The isotach maximum is located within the relatively weak pressure gradient between these two features. The composite pressure tendency pattern indicates that sea level pressure during the previous 12 h rose across the analysis region, with substantial rises found immediately north and northwest of the jet core. This pattern suggests that, keeping in mind the coarse spatial and temporal resolution of this analysis, isallobaric forcing is not an important factor in the formation of Ac-EW jets.

In keeping with the weak composite-pressure gradient, the geostrophic contribution to the actual wind is considerably less than the ageostrophic (Fig. 3). Interestingly, the largest geostrophic wind vectors are not located within the isotach maximum. Rather, two centers of relatively strong vectors are evident—one to the east and another to the south of the jet core. In contrast, the ageostrophic component is fairly strong in the vicinity of the jet core, although the largest composite ageostrophic wind vectors are displaced somewhat to the west and south of the isotach maximum. An interesting observation is the veering of the ageostrophic wind vectors with latitude through the jet core, possibly due to transverse circulations in the ''exit'' and ''entrance'' regions of the low-level wind maximum, similar to what has been documented for upper-level jets (Sechrist and Whittaker 1979; Uccellini and Johnson 1979). Another feature worth noting is the region of strong easterly ageostrophic vectors in the southern portion of the composite that may reflect a transverse circulation about a dryline.

TABLE 2. Key features of the synoptic and subsynoptic-scale environments of the airflow configuration types.

Jet type	Large-scale environment	Quadrant of 200-mb jet streak above low-level wind max	Key sea level pressure features	Relative strength of geostrophic and ageostrophic wind fields
Ac-EW	Quiescent	Right entrance	Col, anticyclone NW of jet core is the strongest feature	Ageostrophic $>$ geostrophic
Ac-SWNE	Quiescent	Right exit	Col, anticyclone SE of the jet core is the strongest feature	Geostrophic $>$ ageostrophic
Kc-SWNE	Active	Right entrance	SW–NE-oriented trough with closed isobar N of the jet core	Geostrophic $\cong$ ageostrophic
Bd-SWNE	Active	Right entrance	SW–NE-oriented trough with closed isobar SW of the jet core	Geostrophic $\cong$ ageostrophic
Bd-NWSE	Active	Right entrance	N–S-oriented trough	Geostrophic $\cong$ ageostrophic
Cc	Active	Two jet streaks	N–S-oriented trough	Ageostrophic $>$ geostrophic
LAc-SWNE	Active	Unclear	Anticyclone E of jet core	Geostrophic $>$ ageostrophic
L2A	Active	Right entrance	Ridge of surface high pressure E of jet core	Geostrophic $>$ ageostrophic
LBKc-SWNE	Active	Right entrance	SW–NE oriented trough	Geostrophic $>$ ageostrophic
LB	Active	Right entrance	Surface trough W of jet core; anticyclone to E	Geostrophic $\cong$ ageostrophic
LKc-SWNE	Active	Right entrance	Surface cyclone SW of the jet core; anticyclone to E	Geostrophic $>$ ageostrophic
LCC	Active	Two jet streaks	N–S-oriented surface trough W of the jet core; anticyclone to NE	Geostrophic $\cong$ ageostrophic

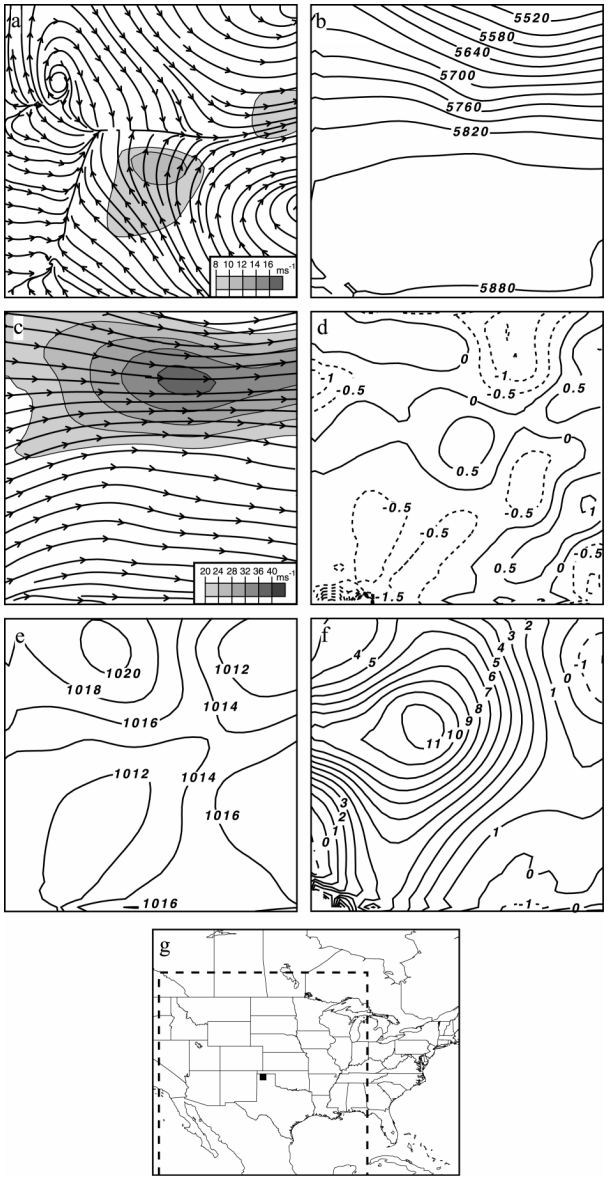

FIG. 2. Composite patterns for Ac-EW jets: (a) isotachs (m s^{-1}) and streamlines for the lowest constant-pressure surface with a jet ''nose'' (i.e., level 1), (b) 500-mb geopotential height (m), (c) 200-mb isotachs (m s^{-1}) and streamlines, (d) divergence at 200 mb (10^{-5} s^{-1}; negative dashed), (e) sea level pressure (mb), (f) 12-h sea level pressure tendency (mb), and (g) a representative subgrid centered on the median location of Ac-EW jets.

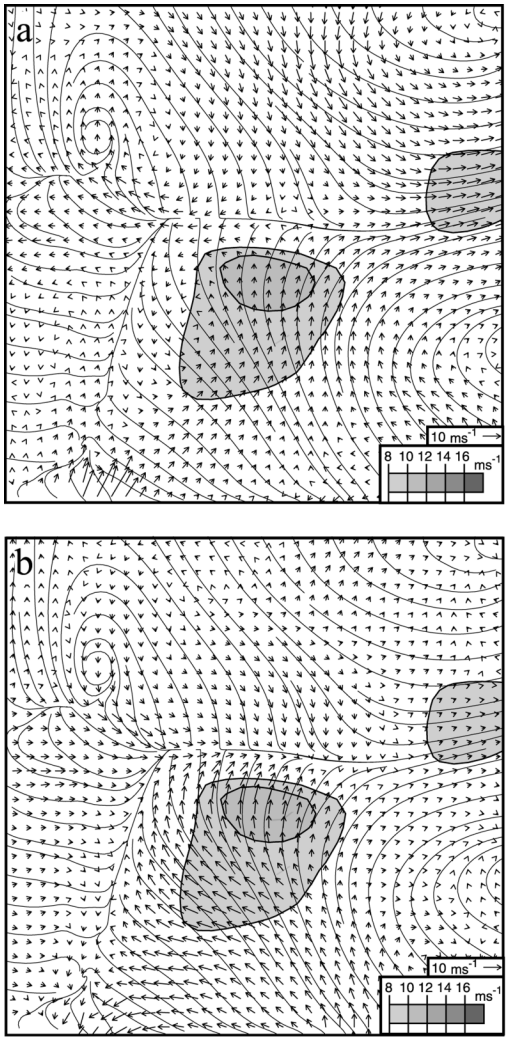

FIG. 3. Composite (a) geostrophic wind vectors and (b) ageostrophic wind vectors overlaid onto a simplified isotach-streamline plot for Ac-EW jets. The vectors are plotted on a 1° lat by 1° long grid.

b. Anticyclonically curved wind maximum with confluence zone oriented southwest–northeast (Ac-SWNE jets)

Ac-SWNE jets are also typically located under a 500-mb ridge (i.e., a quiescent environment), although the ridge is better defined compared to that for Ac-EW jets (Fig. 4). Surprisingly, Ac-SWNE jets are directed toward the right exit quadrant of a 200-mb jet streak. This quadrant is generally considered a region of upper-level convergence. However, the composite 200-mb divergence field is weak and neither convergence nor divergence is indicated in the vicinity of the jet streak.

A col in the sea level pressure composite is also evident for Ac-SWNE jets. However, the anticyclone and cyclone located to the northwest and to the northeast, respectively, of the wind maximum are considerably weaker than similar features for Ac-EW jets. The dominant surface pressure feature is an anticyclone southeast of the jet axis. Ac-SWNE jets are embedded within the return flow around this anticyclone (i.e., the Bermuda high). The isotach maximum is located near the western edge of a surface pressure gradient that is considerably stronger than the gradient observed for Ac-EW jets. The composite pressure tendency pattern suggests that surface pressure has increased slightly over the analysis region during the previous 12 h.

In contrast to the Ac-EW jets, the geostrophic wind

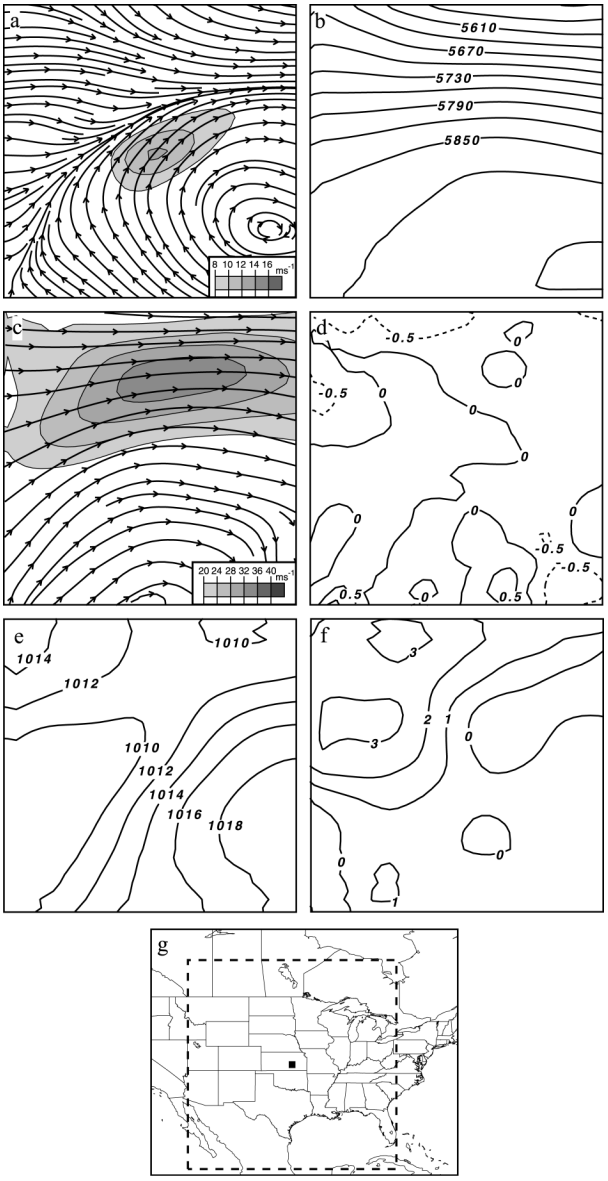

FIG. 4. Same as in Fig. 2 except for Ac-SWNE jets.

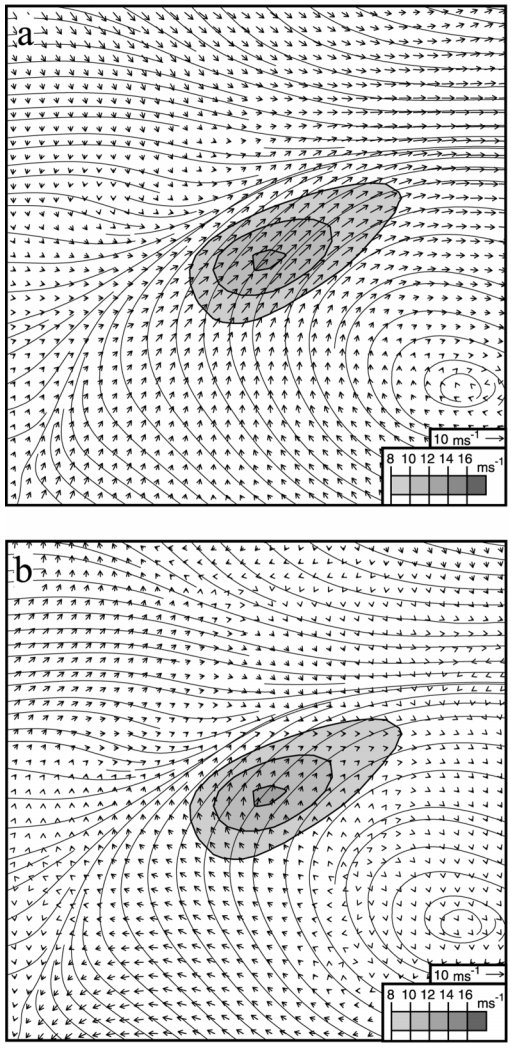

FIG. 5. Same as in Fig. 3 except for Ac-SWNE jets.

component is greater than the ageostrophic for Ac-SWNE jets (Fig. 5). The area of largest geostrophic wind vectors coincides with the location of the isotach maximum, suggesting that the local maximum in the pressure gradient is an important forcing mechanism. For the most part, the geostrophic vectors are aligned with the composite streamlines. It is interesting to note that, similar to Ac-EW jets, two centers of relatively strong ageostrophic wind vectors are present for Ac-SWNE jets. One center is found in the southern portion of the composite grid. The second center is found in the vicinity of the isotach maximum, where the ageostrophic wind vectors are generally directed toward the confluence zone to the west of the jet axis. As for Ac-EW jets, the direction of the ageostrophic component veers with latitude through the isotach maximum.

c. Wind maximum with closed cyclonic circulation (kurl) and confluence oriented southwest–northeast (Kc-SWNE jets)

The synoptic-scale environment of Kc-SWNE jets differs substantially from that of the two previously discussed airflow types in that the wind maximum is located downstream of a weak trough on the composite 500-mb surface rather than near the axis of a ridge (Fig. 6). In other words, Kc-SWNE jets are typically associated with an active environment. The composite 200-mb wind field suggests that Kc-SWNE jets are directed toward the right entrance quadrant of an upper-level jet streak. A local maximum in the 200-mb composite divergence field is found immediately downstream of the jet core for Kc-SWNE jets.

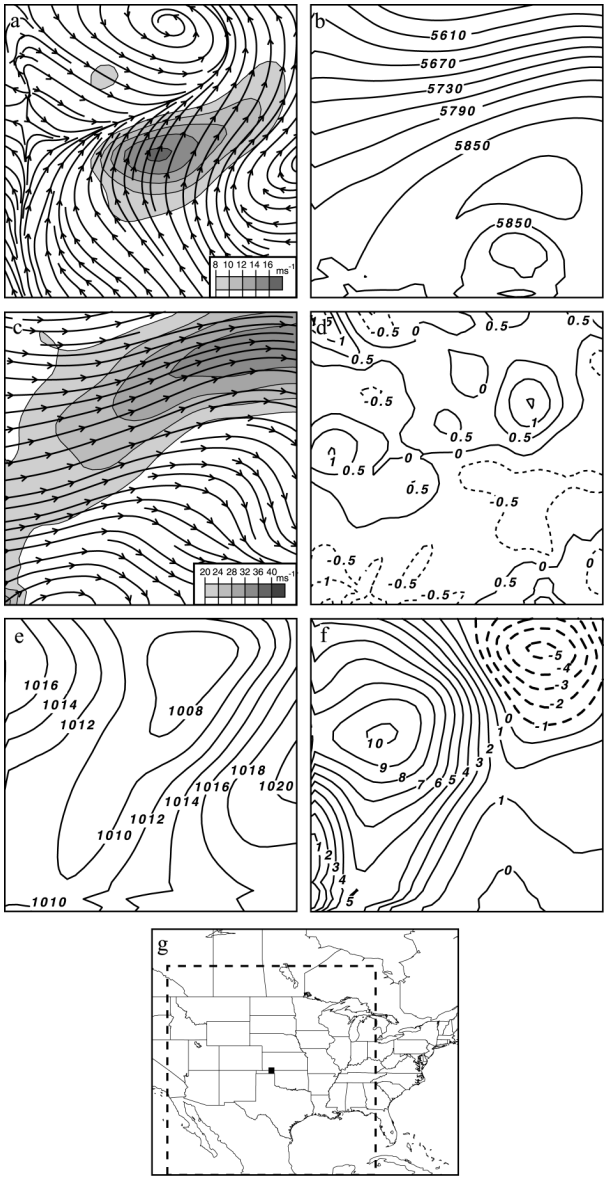

FIG. 6. Same as in Fig. 2 except for Kc-SWNE jets.

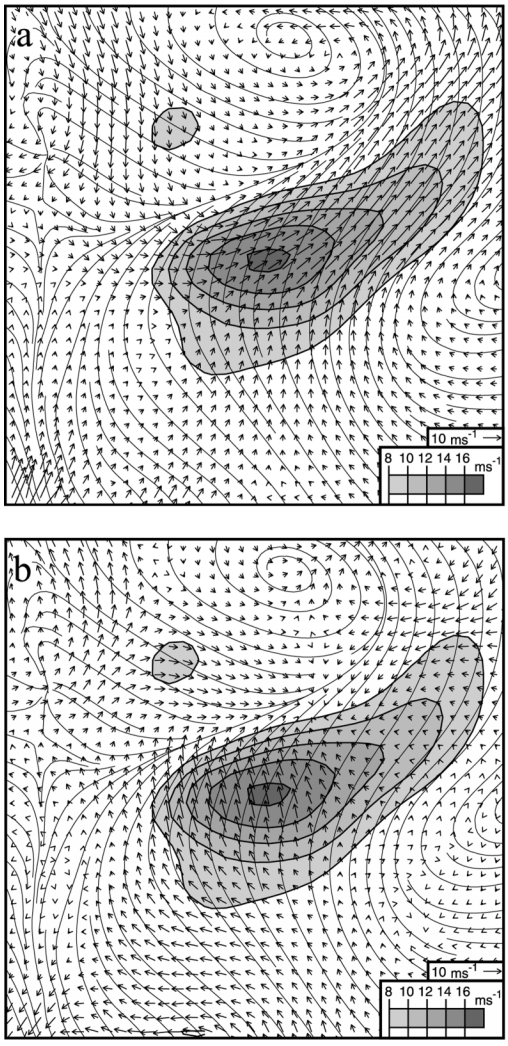

FIG. 7. Same as in Fig. 3 except for Kc-SWNE jets.

The composite sea level pressure pattern is dominated by an elongated trough with a southwest–northeast orientation, rather than by a col as was the case for the previous two jet types. The lowest average pressure, indicated by a closed isobar within the trough, is located north of the jet core. Two anticyclones, one in the extreme eastern, and another in the northwestern portion of the analysis region, are evident in the composite pressure map. The composite pressure tendency field suggests that the northwestern anticyclone strengthened in the previous 12 h, whereas pressure fell over the northeastern portion of the analysis region.

The comparatively strong pressure gradient along the eastern edge of the composite area corresponds with a relatively strong geostrophic wind component, although the largest geostrophic vectors are displaced east and north of the jet core (Fig. 7). On the other hand, large ageostrophic wind vectors are found in the vicinity of the isotach maximum. Apparently, the pressure gradient can ''set the stage'' for the formation of Kc-SWNE jets, but the ageostrophic component is important in determining the location of the isotach maximum. The ageostrophic vectors are directed toward the southwest–northeast-oriented confluence zone. Thus, it appears that the confluence zone may play an important role in generating the ageostrophic wind component. The large-scale pressure falls in the northeastern portion of the analysis area do not appear to be contributing to a strengthening of the low-level wind maximum. Instead, the easterly ageostrophic vectors in this area have a nearly opposite orientation to the southwesterly geostrophic vectors aligned with the pressure gradient. A rotation of the ageostrophic vectors with latitude through the jet core is again evident, and, as seen for the previous types,

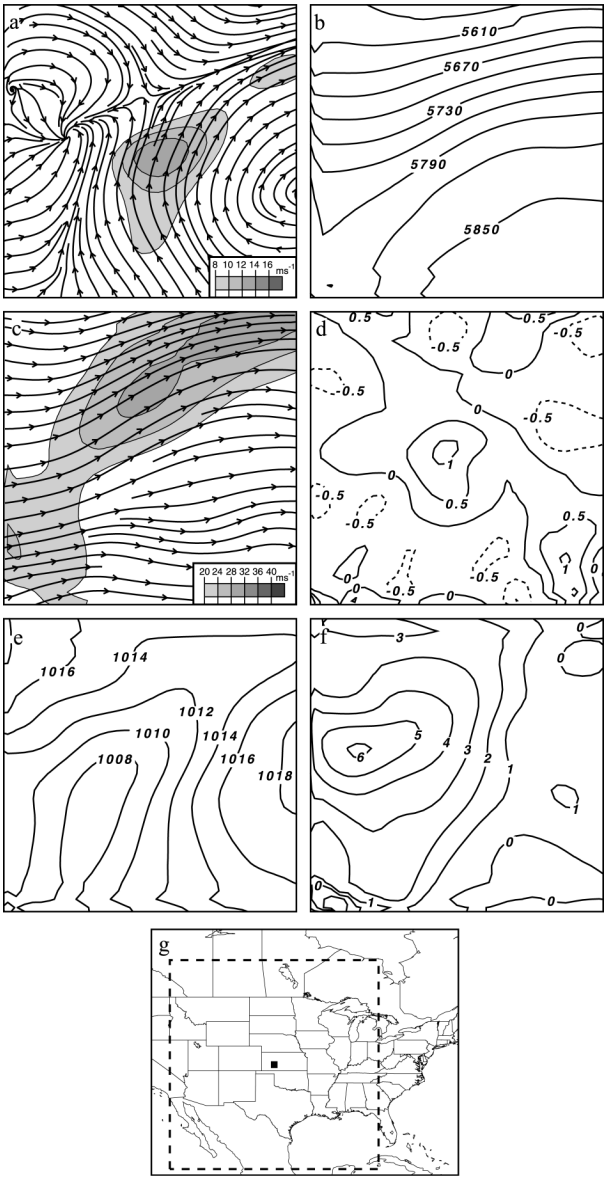

FIG. 8. Same as in Fig. 2 except for Bd-SWNE jets.

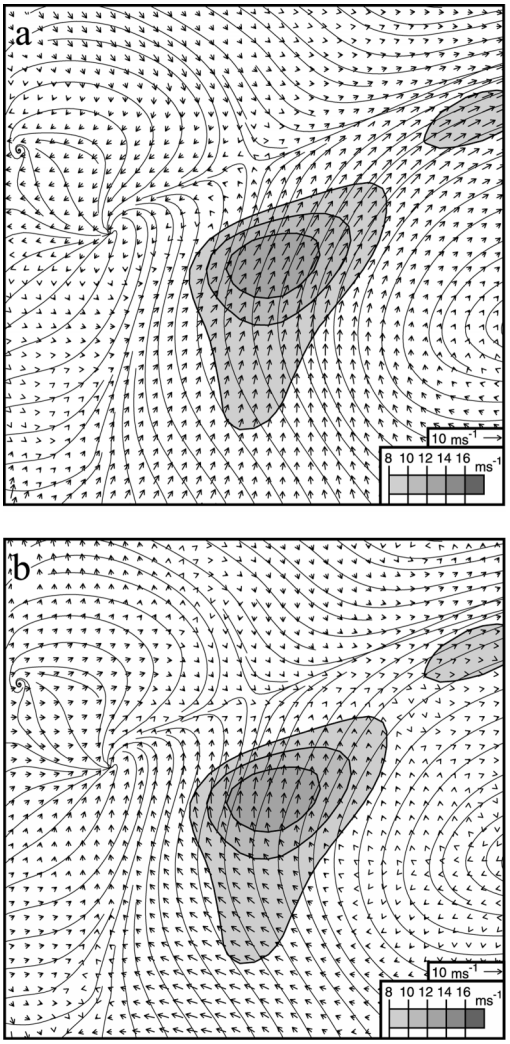

FIG. 9. Same as in Fig. 3 except for Bd-SWNE jets.

relatively large easterly ageostrophic vectors are found in the extreme southern portion of the analysis region.

d. Low-level wind maximum with bifurcating flow and deformation zone oriented southwest–northeast (Bd-SWNE jets)

A composite 500-mb trough is located in the western portion of the analysis region for Bd-SWNE jets, and a ridge is located to the east (Fig. 8). This pattern is similar to that for the previously described Kc-SWNE jets, except that the composite features are somewhat more amplified for Bd-SWNE events. The right entrance region of a 200-mb jet streak, and a resulting area of upper-level divergence, are located immediately north-northwest of the low-level isotach maximum. This composite pattern suggests a linkage between the upper-level jet and the left or westernmost branch of the Bd-SWNE jets.

A southwest–northeast-oriented surface trough covers much of the composite region. The lowest pressure is found southwest of the jet core. The pressure tendency composite is dominated by pressure rises, particularly to the west of the isotach maximum. The jet core is found along the western edge of a pressure gradient that is comparable in strength to the gradients observed for Kc-SWNE and Ac-SWNE jets.

The composite geostrophic wind vectors for Bd-SWNE jets are relatively large, as expected given the comparatively strong surface pressure gradient (Fig. 9). There is also good agreement between the location of the largest geostrophic wind vectors and the isotach maximum. A relatively large ageostrophic component

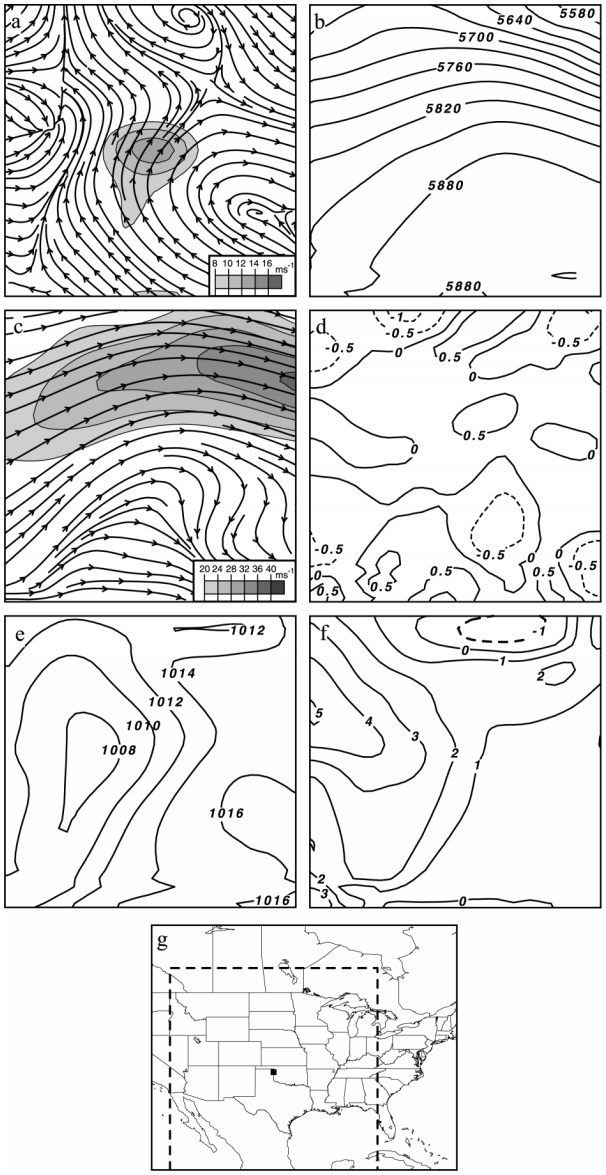

FIG. 10. Same as in Fig. 2 except for Bd-NWSE jets.

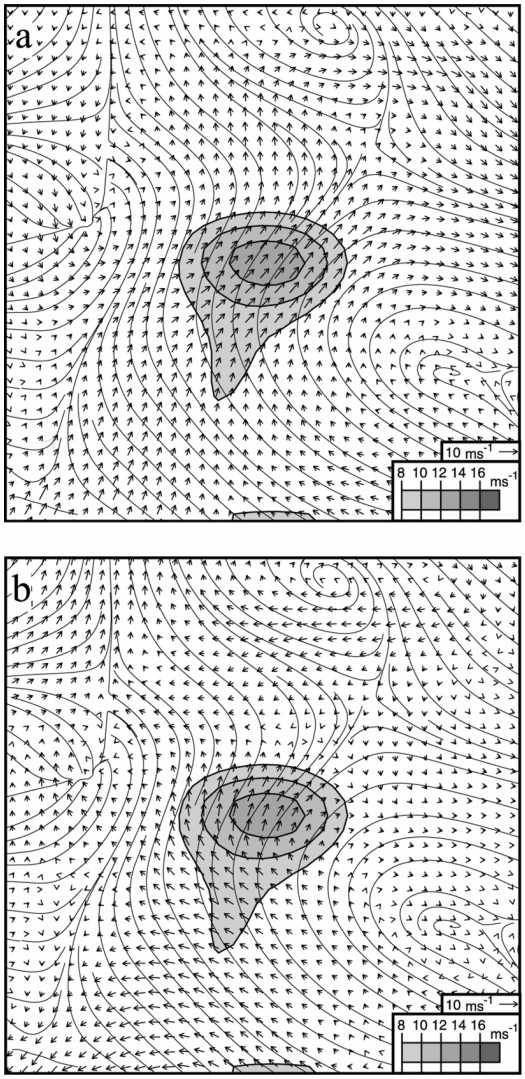

FIG. 11. Same as in Fig. 3 except for Bd-NWSE jets.

is also evident in the vicinity of the isotach maximum, leading to supergeostrophic wind speeds. The ageostrophic vectors in this area are directed toward an east–west-oriented temperature gradient located west and northwest of the jet core (shown in Part I). As for the previous types, the ageostrophic vectors veer with latitude, particularly upstream of the jet core. The bifurcation of Bd-SWNE jets introduces complexities in interpreting the geostrophic and ageostrophic wind fields. The largest geostrophic wind vectors are associated with the right, or eastern, branch, whereas the ageostrophic component is equally large for the right and left branches. Also, both the geostrophic and ageostrophic components are weak in the vicinity of the deformation zone north of the jet core.

e. Low-level wind maximum with bifurcating flow and deformation zone oriented northwest–southeast (Bd-NWSE jets)

The composite 500-mb geopotential height field for Bd-NWSE jets displays a strong ridge over most of the composite area with some evidence of a short-wave trough to the extreme west (Fig. 10). The relatively strong height gradient in the northern portion of the composite grid is associated with fairly strong upper-level winds. Bd-NWSE jets are located underneath the right entrance region of a 200-mb jet streak. The largest upper-level divergence is found in the vicinity of the bifurcation in the low-level wind field.

A trough of surface low pressure is located to the west of the axis of Bd-NWSE jets. This trough has a more north–south orientation compared to the pressure troughs observed for several of the previous types. An anticyclone is present in the southeastern portion of the

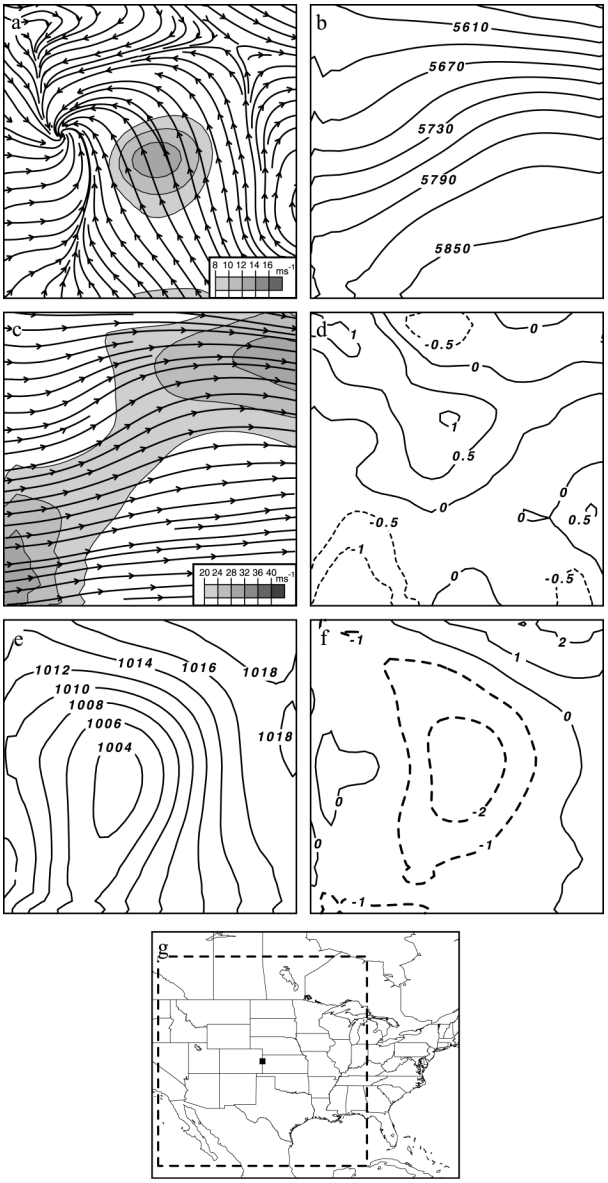

FIG. 12. Same as in Fig. 2 except for Cc jets.

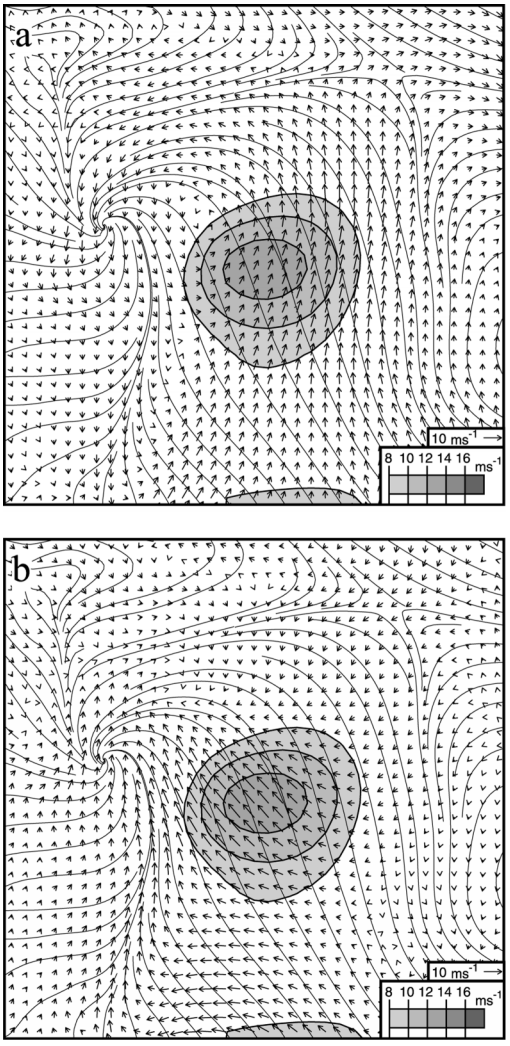

FIG. 13. Same as in Fig. 3 except for Cc jets.

composite region, as was the case for all the previous types. The pressure tendency composite is dominated by modest pressure rises over the majority of the analysis region.

Similar to the other bifurcating jet type (i.e., Bd-SWNE jets), the geostrophic and ageostrophic components are of approximately equal magnitude for Bd-NWSE jets (Fig. 11). The largest geostrophic wind vectors are collocated with the composite isotach maximum, and in general are aligned along the composite streamlines. The ageostrophic wind vectors are also strongest near the jet core. Similar to the other types, the ageostrophic vectors rotate with latitude through the jet core, and, in the southern portion of the composite region the ageostrophic wind vectors are deflected toward the west.

f. Cyclonically curved wind maximum with confluence zone (Cc jets)

The composite 500-mb heights for Cc jets display a trough–ridge pattern (Fig. 12) similar to that observed for the Bd-SWNE jet type. The jet core is observed downstream of the trough axis. The low-level wind maximum is directed toward the right entrance quadrant of an upper-level jet streak and an area of upper-level divergence. However, the 200-mb airflow composite is somewhat more complex than that for the previous jet types in that a second upper-level jet streak is observed in the extreme southwestern portion of the analysis region. At the time of the composite, it is not clear what impact this jet streak has on the low-level wind maximum.

The 500-mb trough supports a large, fairly intense

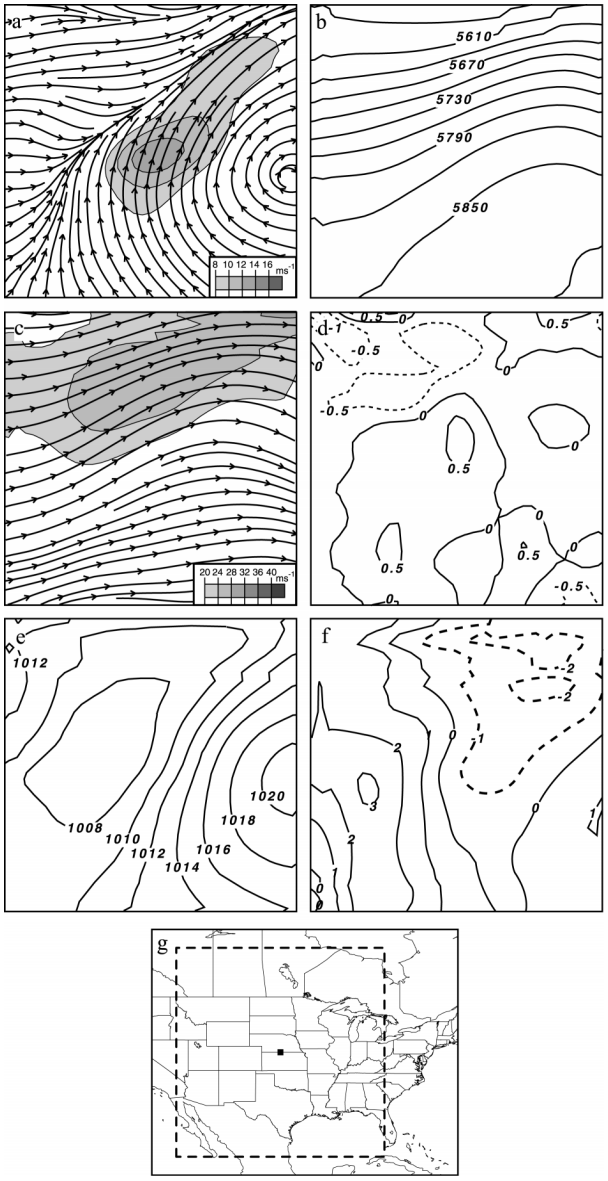

FIG. 14. Same as in Fig. 2 except for LAc-SWNE jets.

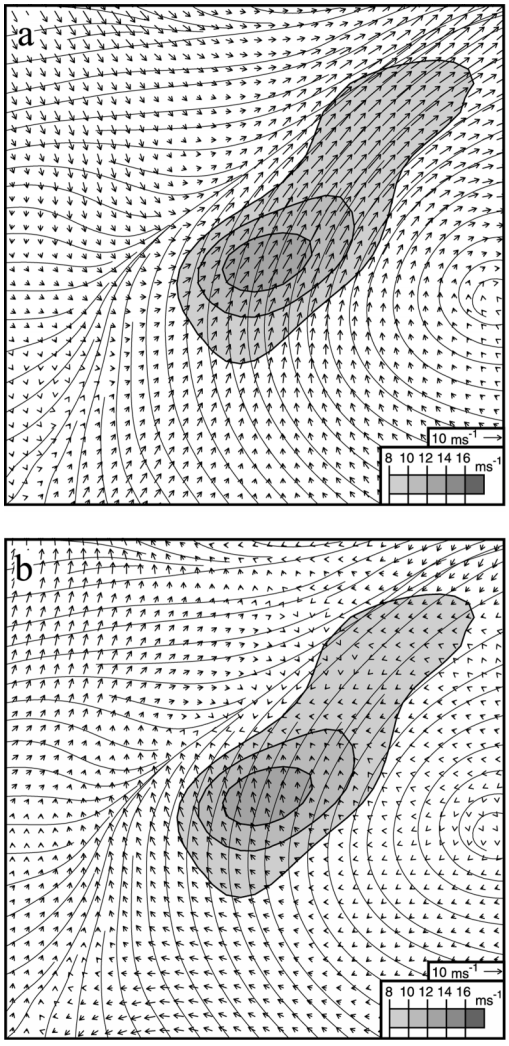

FIG. 15. Same as in Fig. 3 except for LAc-SWNE jets.

surface trough, which is the dominant feature of the sea level pressure composite. The eastern anticyclone, a key feature of the sea level pressure composites for the previous jet types, is confined to the extreme eastern portion of the composite area and is shifted farther north such that the anticyclone center is located at approximately the same latitude as the isotach maximum. The composite jet core is located along the western edge of a relatively strong pressure gradient. The changes in the pressure pattern during the previous 12 h differ significantly from the previous airflow configuration types. In particular, the isotach maximum is located in an area that, on average, experienced pressure falls of 2 mb in the previous 12 h.

Despite the strong pressure gradient, the ageostrophic wind speeds for Cc jets still exceed the geostrophic wind speeds (Fig. 13). The local maximum of the geostrophic wind is displaced to the east and north of the isotach maximum. The strongest ageostrophic wind vectors are observed to the left (west) of the isotach maximum. This area coincides with the large-scale pressure falls evident on the pressure tendency composite. Compared to previous types, the rotation of the ageostrophic wind vectors is less pronounced upstream, and absent downstream, of the jet core. Relatively strong easterly ageostrophic vectors are again present in the southern portion of the analysis area.

g. Long wind maximum with anticyclonic curvature and confluence zone oriented southwest–northeast (LAc-SWNE jets)

LAc-SWNE jets can be considered the ''long'' counterpart of Ac-SWNE jets, in that both types have simple, anticyconically curved airflow. However, the larger lat-

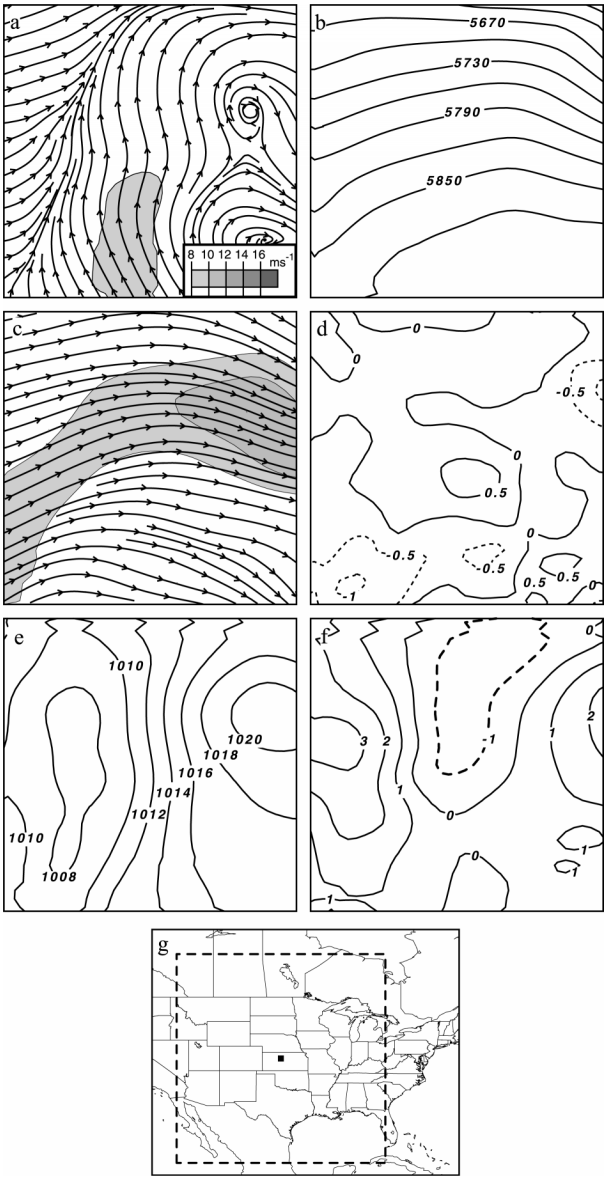

FIG. 16. Same as in Fig. 2 except for L2A jets.

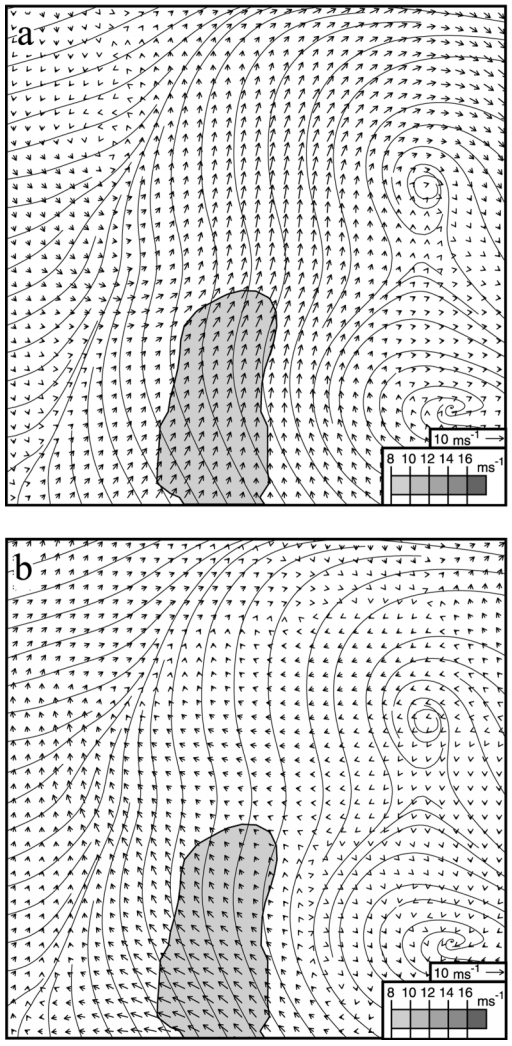

FIG. 17. Same as in Fig. 3 except for L2A jets.

itudinal extent of LAc-SWNE jets implies that they have greater mid- and upper-tropospheric support, and this contention is borne out by the composite analyses. LAc-SWNE jets are located downstream of the axis of a 500-mb trough, whereas Ac-SWNE jets were located near a 500-mb ridge axis. Also, the isotach maximum for LAc-SWNE jets is located under a local maximum in the 200-mb composite divergence field (Fig. 14).

The strongest composite surface feature for LAc-SWNE jets is an anticyclone over the eastern portion of the analysis region. The center of this anticyclone is located at approximately the same latitude as the composite isotach maximum. A southwest–northeast oriented trough of low pressure is located to the west of the jet axis. The isotach maximum for LAc-SWNE jets is located along the western edge of the strongest pressure gradient. The pressure tendency composite indicates that surface pressure has fallen over the previous 12 h to the north and northeast of the isotach maximum.

The geostrophic wind component is stronger than the ageostrophic component for LAc-SWNE jets (Fig. 15). The strongest geostrophic wind speeds are found north and east of the isotach maximum, where the composite pressure gradient is strongest. In this area, the geostrophic wind vectors are aligned with the actual wind. The composite geostrophic vectors are also fairly large in the vicinity of the isotach maximum, although here the direction of the vectors is more southwesterly compared to the actual wind. On the other hand, the ageostrophic vectors in the vicinity of the isotach maximum have a southeasterly direction and are oriented toward the confluence zone west of the jet axis. Compared to many of the previous types, a distinct veering of the ageostrophic vectors with latitude is not evident for LAc-SWNE jets. However, a relatively large easterly

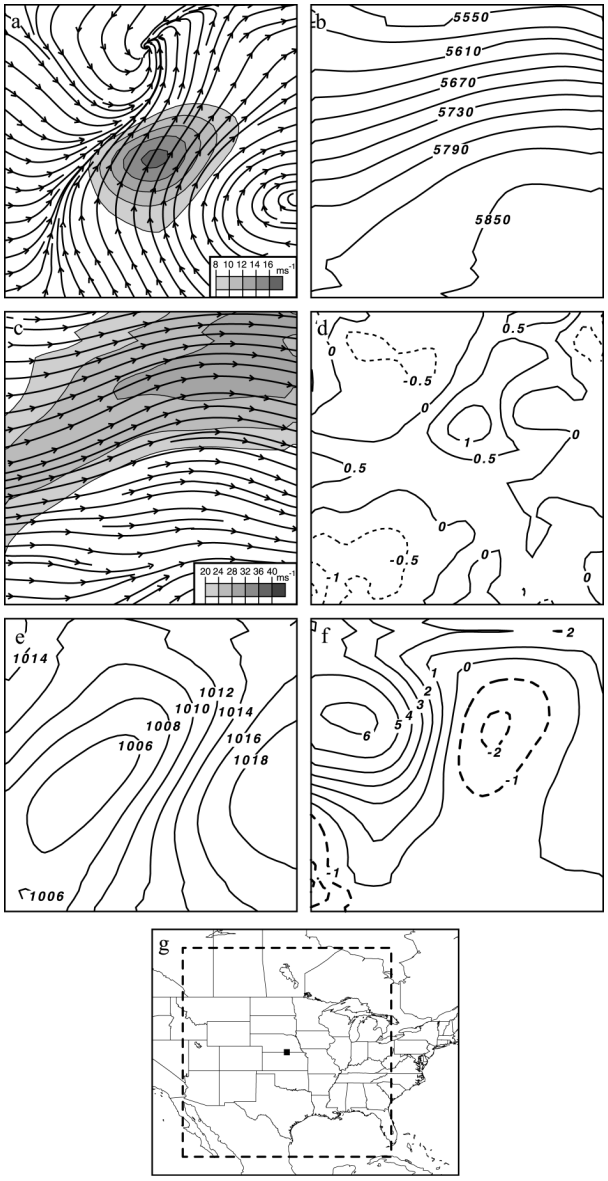

FIG. 18. Same as in Fig. 2 except for LBKc-SWNE jets.

ageostrophic component is again found in the southern portion of the analysis region.

h. Long wind maximum with two anticyclonic circulation centers (L2A jets)

As described in Part I, the airflow of L2A jets consists of two closed anticyclonic circulation centers, and the jet core is found either to the west of the northern closed circulation, to the west of the southern closed circulation, or in between the two centers. In order to preserve the airflow configuration, the wind maxima were composited relative to the two closed circulations rather than with respect to the jet core. Consequently, the center of the composite map does not reflect the median location

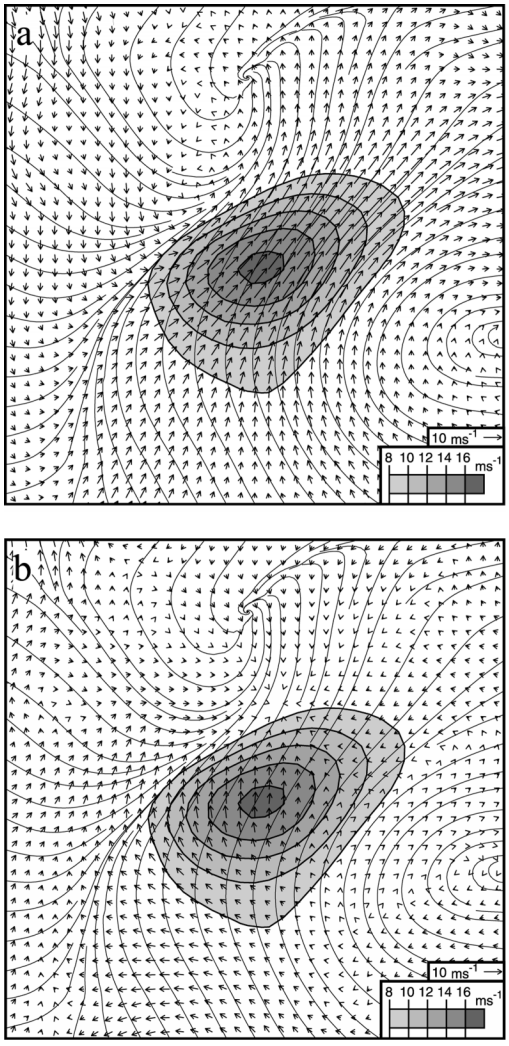

FIG. 19. Same as in Fig. 3 except for LBKc-SWNE jets.

of the jet core, as it does for the other configuration types. Bearing this caveat in mind, L2A jets are typically associated with a weak trough in the extreme western portion of the analysis region and an upper-level ridge over the eastern two-thirds of the region (Fig. 16). L2A jets tend to be located south of the right entrance region of a 200-mb jet streak. A local maximum in the composite 200-mb divergence field is evident immediately downstream of the low-level wind maximum.

The upper-level ridge supports an extensive ridge of surface high pressure across the eastern portion of the composite map. The northern portion of this ridge is more intense, as indicated by the closed isobars (average central pressure of 1020 mb). Note that the closed anticyclonic circulation on the streamline composite agrees well with the location of the center of the northern high. The pressure ridge is not as strong to the south, and a closed isobar is not present. Another important feature is the north–south-oriented low pressure trough (average central pressure of 1008 mb) across the western

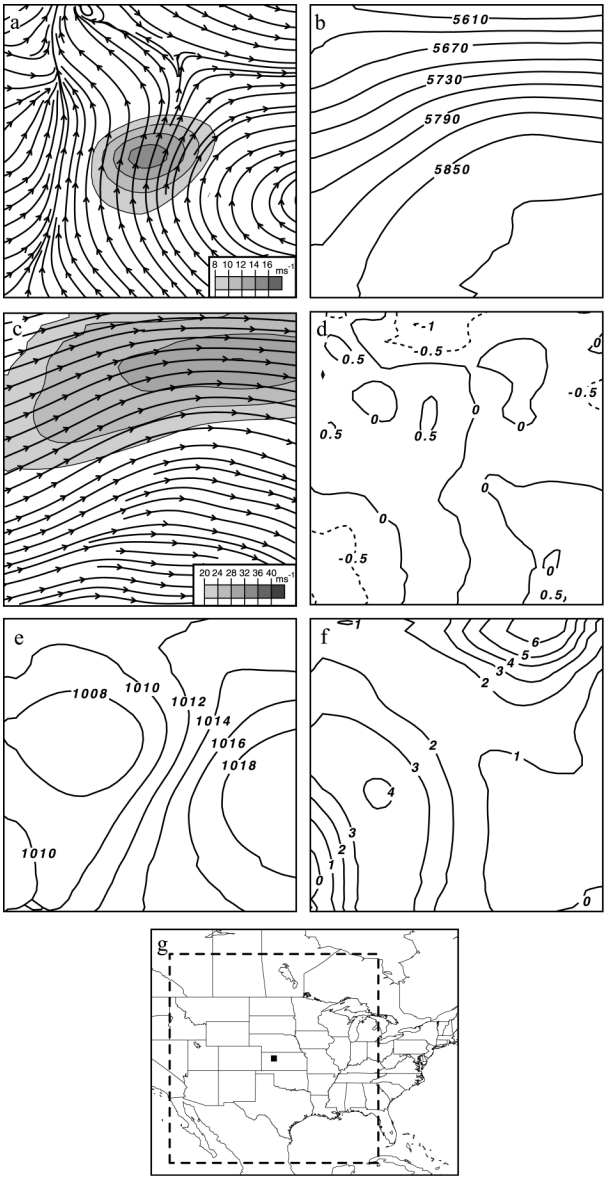

FIG. 20. Same as in Fig. 2 except for LB jets.

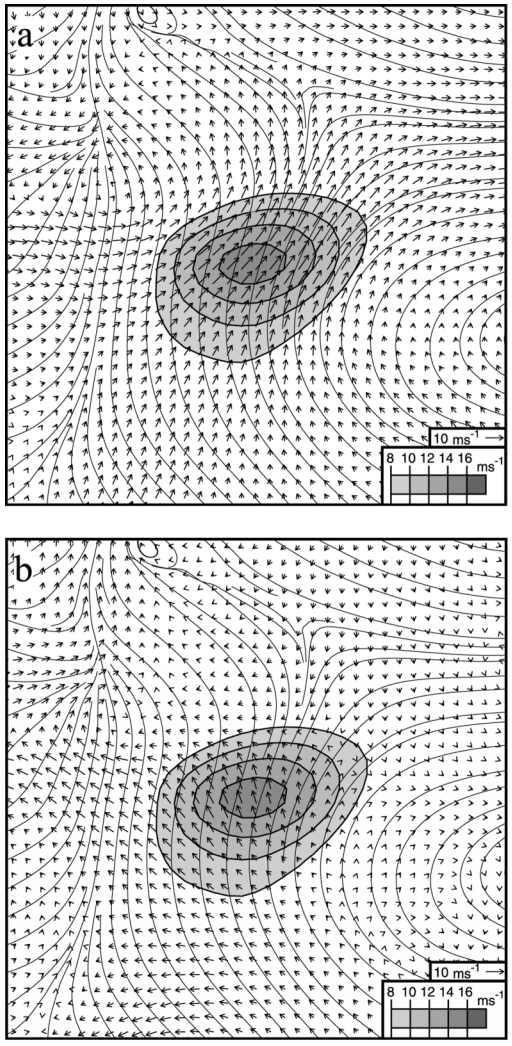

FIG. 21. Same as in Fig. 3 except for LB jets.

portion of the composite. A relatively strong pressure gradient exists between the latitudinally extensive eastern ridge and the western trough. Small-to-modest pressure falls are seen immediately east of the surface trough, whereas modest pressure rises are observed over the extreme western and eastern portions of the analysis region.

The composite geostrophic wind component is considerably stronger than the ageostrophic component for L2A jets (Fig. 17). The largest geostrophic vectors are found along and to the east of the jet axis, where the composite pressure gradient is greatest. The only area of relatively large ageostrophic vectors is found in the extreme southern portion of the analysis region.

i. Long bifurcating wind maximum with kurl and confluence zone oriented southwest–northeast (LBKc-SWNE jets)

The next airflow configuration, LBKc-SWNE jets, is the long counterpart of the Kc-SWNE jets, and, similar to Kc-SWNE jets, the midtropospheric environment appears to play a role in the development of this low-level wind maximum. The composite 500-mb geopotential height field is nearly identical to that for the Kc-SWNE jets with a trough in the west and a ridge in the east (Fig. 18). Also, like Kc-SWNE jets, LBKc-SWNE jets are located underneath the right entrance region of a 200-mb jet, although the average 200-mb divergence is somewhat larger for LBKc-SWNE jets. The low-level jet is directed toward the local maximum in the upper-level divergence field.

The midtropospheric trough supports a southwest–northeast-oriented surface pressure trough located to the west of the jet axis. An anticyclone is evident in the

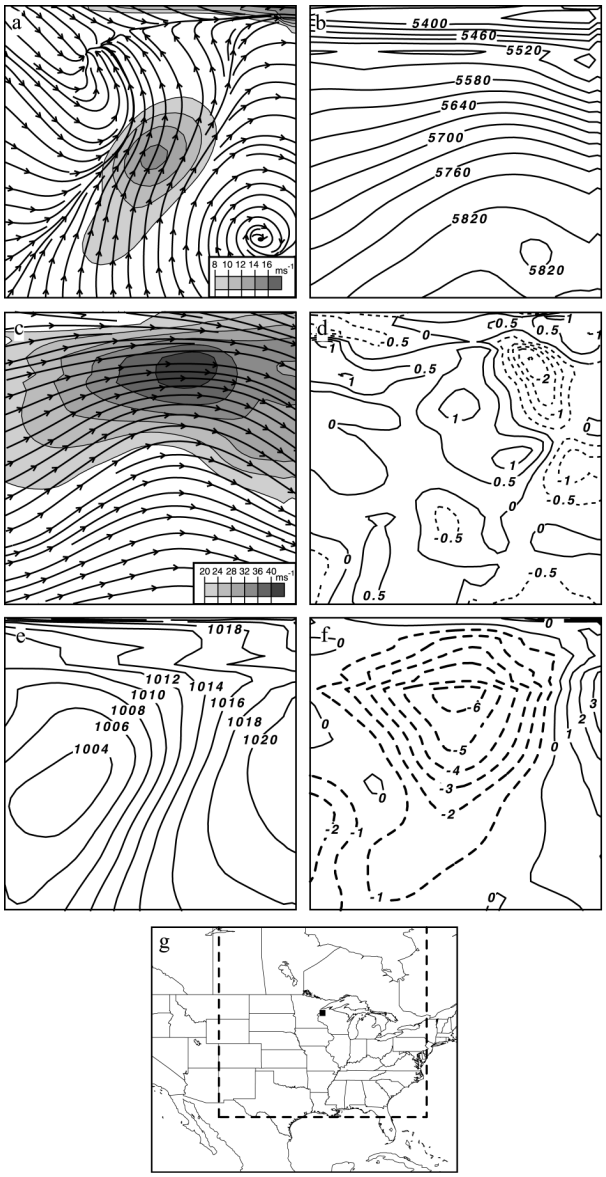

FIG. 22. Same as in Fig. 2 except for LKc-SWNE jets.

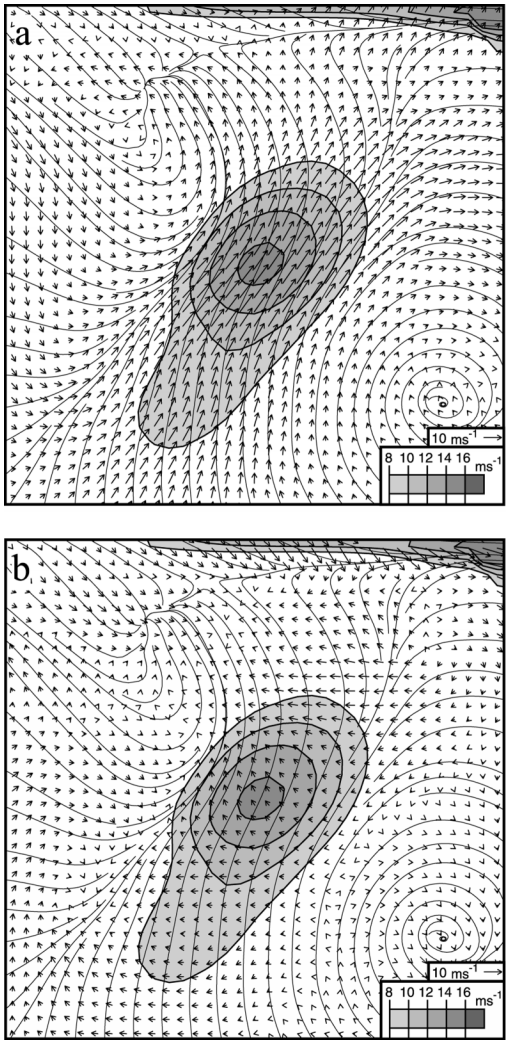

FIG. 23. Same as in Fig. 3 except for LKc-SWNE jets.

eastern portion of the composite sea level pressure field. The strength of the pressure gradient between these two features is comparable to that for Kc-SWNE jets. One difference between the two types, however, is the location of the closed isobar within the surface pressure trough. For the LBKc-SWNE jets, the closed isobar is found to the west-southwest of the jet axis, whereas for the Kc-SWNE jets it is located north-northeast of the jet core. For both types, pressure rises over the past 12 h are found west and northwest of the jet axis, although the average values are not as large for the LBKc-SWNE jets. Average pressure falls are also smaller for the LBKc-SWNE jets, and compared to Kc-SWNE jets, the area of greatest pressure falls is displaced southward, closer to the isotach maximum.

In spite of the similarities in the composite sea level pressure fields for the two types, the geostrophic and ageostrophic wind fields differ (Fig. 19). For both types, the strongest geostrophic wind vectors are located over and to the northeast of the jet core. However, the vectors for the LBKc-SWNE jets have a southwesterly orientation compared to a more westerly orientation for the Kc-SWNE jets. Also, the ageostrophic component is weaker than the geostrophic component for LBKc-SWNE jets, whereas the ageostrophic and geostrophic component for Kc-SWNE jets are of similar magnitudes. For the LBKc-SWNE jets, the ageostrophic component in the vicinity of the jet core is directed toward the north, whereas it is directed toward the northwest for Kc-SWNE jets. Also, there does not appear to be as strong a connection for LBKc-SWNE jets as there is for Kc-SWNE jets between the orientation and magnitude of the ageostrophic vectors and the location of the confluence zone west of the jet axis. A final difference is that, in contrast to the Kc-SWNE jets, the ageostrophic component for LBKc-

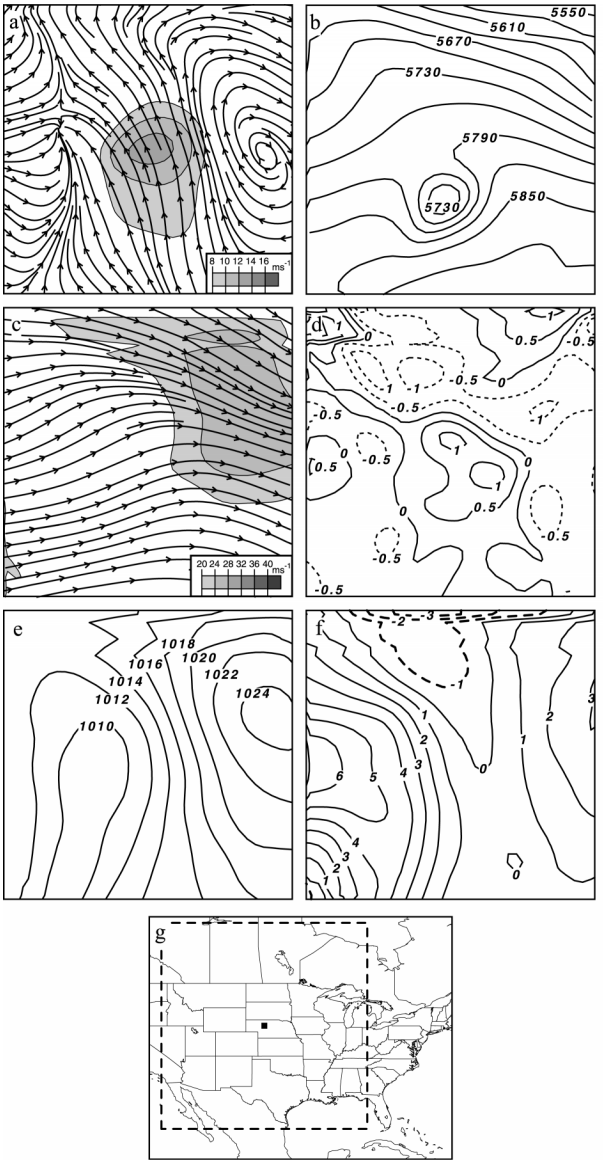

FIG. 24. Same as in Fig. 2 except for LCc jets.

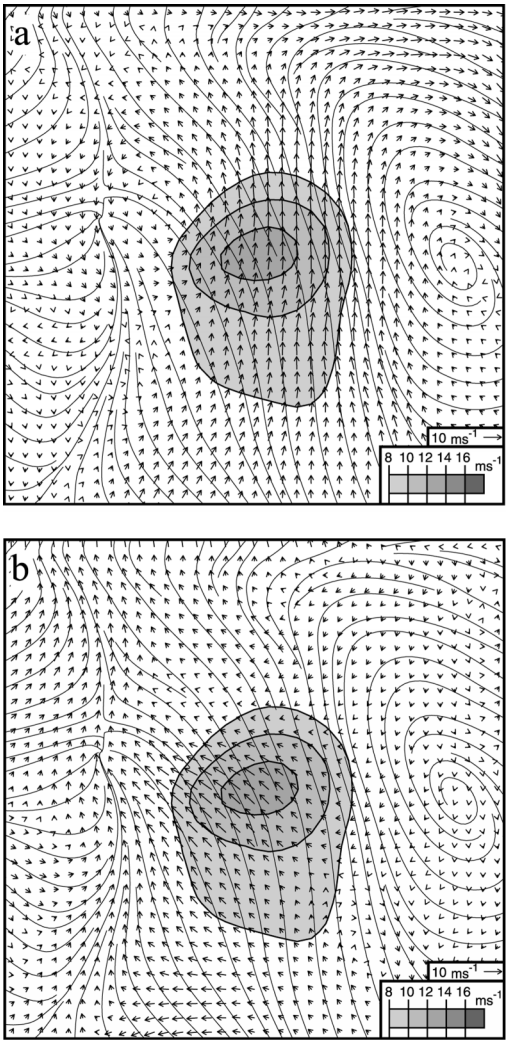

FIG. 25. Same as in Fig. 3 except for LCc jets.

SWNE jets is weak in the vicinity of the largest pressure falls on the composite pressure tendency map.

j. Long bifurcating wind maximum (LB jets)

Similar to the other long types, LB jets are typically located downstream of a 500-mb trough and beneath the right entrance quadrant of a 200-mb jet streak (Fig. 20). The axis of LB jets is found along the western edge of a relatively strong gradient between a surface high pressure system to the east and a surface low pressure system in the western half of the analysis region. The 12-h pressure tendency composite suggests that during the previous 12 h pressure has risen across the analysis region.

The geostrophic and ageostrophic wind components are of approximately equal magnitude for LB jets (Fig. 21), in contrast to the previous three long types where the geostrophic wind was dominant. A distinct bifurcation in the geostrophic wind vectors is evident along the western and eastern branches of the LB jets. Both components are large in the vicinity of the jet core. However the geostrophic vectors are southwesterly, whereas the ageostrophic vectors are southeasterly. In general, the ageostrophic vectors near the isotach maximum are directed toward the low pressure system to the west. Ageostrophic wind vectors are also relatively large in the extreme southern portion of the analysis area. A rotation of the ageostrophic wind vector with latitude is only observed upstream of the jet core.

k. Long wind maximum with kurl and confluence zone oriented southwest–northeast (LKC-SWNE jets)

LKc-SWNE jets are typically located immediately upstream of a 500-mb ridge axis (Fig. 22). Farther up-

stream, a midtropospheric trough is present. Like most previous types, a jet streak is evident in the composite 200-mb wind field. The average speed of this upper-level jet is faster (42 m s^{-1}) than for any other type. The superposition of the upper and lower wind maxima places the low-level jet underneath the right entrance region of the upper-level jet streak. The largest values of upper-level divergence are found immediately north of the isotach maximum.

The composite sea level pressure pattern for LKc-SWNE jets is characterized by a relatively strong low pressure system southwest of the isotach maximum and a comparatively strong anticyclone in the eastern margin of the composite area. The pressure gradient in the vicinity of the isotach maximum is stronger for LKc-SWNE jets than for any other type. The low pressure system appears to have advanced eastward during the previous 12 h, resulting in relatively large pressure falls downstream of the low-level wind maximum.

The geostrophic component of the wind is the dominant contributor to the observed airflow pattern for LKc-SWNE jets (Fig. 23). The strongest geostrophic winds are observed in the vicinity of the isotach maximum. The ageostrophic component for LKc-SWNE jets is considerably smaller than the geostrophic component. As for many of the previous types, the contribution of the ageostrophic to the actual wind consists of a deflection of the actural wind to the left of the geostrophic wind. The strongest ageostrophic wind components are observed to the north and northeast of the isotach maximum. These easterly vectors are directed toward the area of largest 12-h pressure falls. In contrast to the majority of other types, the ageostrophic vectors in the extreme southern portion of the analysis region are relatively small.

l. Long wind maximum with cyclonic flow and confluence (LCc jets)

The final configuration type, LCc jets, have a unique midtropospheric composite pattern (Fig. 24). ''Split flow'' is evident at 500 mb, with a cutoff low embedded in the southern airstream and a ridge evident in the northern airstream. Although an upper-level jet streak is seen in the northeastern portion of the composite 200-mb wind field, the jet streak is considerably weaker than similar features for the other jet types. Nevertheless, the right entrance quadrant appears to be located over and to the east of the low-level wind maximum. A second jet streak is evident in the extreme southwestern corner of the composite grid. The largest mean values of 200-mb divergence are located directly above the core of the low-level wind maximum.

The surface pressure pattern for LCc jets is comparatively simple. A trough of low pressure extends along the western edge of the low-level wind maximum and an anticyclone is evident to the east. The anticyclone is located farther north than similar features for the other types. Another difference is that the ridge of surface high pressure has a northwest–southeast orientation, rather than the north–south or southwest–northeast orientation evident for the other jet types. The jet core is found in its now familiar location—the western edge of the pressure gradient between a high pressure system to the east and a low pressure system to the west. The pressure tendency composite suggests that the sea level pressure pattern has undergone only moderate changes in the previous 12 h. An area of weak pressure falls is evident well north of the isotach maximum.

The mean pressure pattern contributes to an elongated zone of strong geostrophic winds east of the axis of the low-level wind maximum (Fig. 25). Similar to a number of other jet types, the strongest geostrophic wind vectors for LCc jets are not collocated with the isotach maximum. Rather, they are displaced to the northeast. The strongest ageostrophic vectors are confined to either the area just west of the isotach maximum or the southern portion of the analysis region. Within the isotach maximum itself, the geostrophic and ageostrophic components have similar magnitudes, but marked differences in orientation are evident. The geostrophic component is directed toward the north, whereas the ageostrophic component is directed toward the confluence center located northwest of the isotach maximum.

5. Discussion

Previous authors have shown that low-level wind maxima can occur in either a quiescent or an active large-scale environment (Uccellini 1980; Mitchell et al. 1995; Igau and Nielsen-Gammon 1998). Furthermore, some studies suggest that low-level wind maxima are more frequent in an active setting (Uccellini 1980; Mitchell et al. 1995). This study, which employs a large sample of low-level wind maxima, confirms these previous observations. In particular, the composite patterns show that low-level wind maxima occur most frequently with troughing over the southwestern United States (i.e., an active environment). Only 2 (i.e., Ac-EW and Ac-SWNE jets) of the 12 airflow configuration types occur with a midtropospheric ridge (i.e., a quiescent environment).

An additional finding is that low-level wind maxima in quiescent settings have fairly simple, anticyclonically curved airflow. Consequently, the distinct variations in the airflow configuration of low-level wind maxima documented in Part I occur in active midtropospheric environments. Also, the type of environment, active or quiescent, exerts an influence on the latitudinal extent of the individual jet types. The results presented here suggest that jets that form in a quiescent environment have limited latitudinal extents, whereas the latitudinal extents of jets that occur in an active environment vary from small to large.

There are some features that low-level jets in quiescent and active environments have in common. One

characteristic present for the majority of the jet types is an area of large ageostrophic wind vectors to the northwest of the jet core. In general, these vectors point toward a confluence boundary along the left (west) flank of the low-level wind maxima. The enhanced ageostrophic wind is possibly the result of an isallobaric component in connection with changes in the strength of the confluence/frontal zone, or, alternatively, of the conversion of pressure gradient forcing to kinetic energy (Bonner et al. 1968). The orientation of the ageostrophic vectors is also suggestive of a transverse circulation about the confluence/frontal zone. For the majority of jet types, a second area of strong ageostrophic wind vectors is found to the south of the jet core, in an area with a marked moisture gradient. In this case, the ageostrophic vectors are likely a reflection of a transverse circulation about a dryline (Ziegler and Hane 1993).

A characteristic of almost all jet types is veering (i.e., anticyclonic rotation) of the ageostrophic wind vectors with latitude upstream of the jet core. Veering of the ageostrophic vectors was also observed downstream of the jet core for a few types (i.e., Ac-EW, Ac-SWNE, Bd-SWNE, Bd-NWSE jets). A possible explanation for the change in direction of the ageostrophic component might be transverse circulations associated with the low-level wind maximum itself. Transverse circulations around upper-level jet streaks have been widely documented (Sechrist and Whittaker 1979; Uccellini and Johnson 1979), and a similar circulation has been speculated upon, but not documented, for lower-tropospheric jets (e.g., Kotroni et al. 1994).

For the majority of the jet types, the right entrance quadrant of an anticyclonically curved 200-mb jet streak and associated upper-level divergence are superimposed upon an area of low-level speed convergence downstream of the low-level wind maxima. Even Ac-EW jets that form in a quiescent setting and would be expected to have little linkage with the upper troposphere share this feature. Interestingly, for the jet types with bifurcating flow, the upper-tropospheric divergence is generally located over the left (west) branch of the bifurcating jet. Two exceptions to the right entrance quadrant ''rule'' are the Ac-SWNE jets which appear to be located under the right exit quadrant of an upper-tropospheric jet, and the LAc-SWNE jets whose relationship to an upper jet streak is not clear. The upper-tropospheric airflow pattern is more complicated for Cc and LCc jets. Two upper-level wind maxima are evident, although it appears that the easternmost jet streak may be more strongly associated with the low-level wind maximum.

The location of the majority of the low-level wind maxima with respect to the right entrance quadrant of upper-level jet streaks is an interesting finding. This quadrant is not commonly associated with strong synoptically forced disturbances, although it has previously been shown to be conducive to the formation of convection (Beebe and Bates 1955; McNulty 1978). Rather, synoptic disturbances have typically been associated with the left exit quadrant of jet streaks (Hovanec and Horn 1975; Uccellini and Johnson 1979; Whittaker and Horn 1981). A similar association was expected in this study, as Uccellini and Johnson (1979) showed that low-level jets under the left exit quadrant of an upper-tropospheric jet streak are embedded within an indirect transverse circulation. This transverse circulation is perpendicular to the upper-level jet and has a lower branch that is directed from south to north. On the other hand, the entrance region of an upper-level jet streak is characterized by a direct circulation with a north–south-oriented lower branch. Thus, while it appears that there may be dynamic support from the superposition of the low-level convergence and upper-level divergence fields, the role of the ageostrophic component resulting from the transverse circulations associated with upper-tropospheric jet streaks is uncertain.

The other characteristics of low-level wind maxima varied considerably between jet types that occur in quiescent and active environments. Some of the key findings are highlighted below.

a. Low-level wind maxima in quiescent environments

As mentioned above, only two jet types, Ac-EW and Ac-SWNE jets, were found to occur in a quiescent mid- and upper-tropospheric environment. In terms of absolute numbers, only 17% of the southerly jet events during the 1991–92 warm seasons fell within these two categories. The small number of jet types, and the relatively small number of events associated with each type, are interesting results, given that the location under an upper-level ridge traditionally has been considered the favorable environment for the formation of low-level wind maxima (Wexler 1961; Hoecker 1965; Bonner 1968).

Previous authors have argued that mesoscale and boundary layer processes govern the development of low-level wind maxima in a quiescent environment (Blackadar 1957; Igau and Nielsen-Gammon 1998). While this study generally supports these earlier findings, it also suggests that, within a quiescent setting, the relative influence of boundary layer processes varies for wind maxima with different airflow configurations. Despite the close similarities of the midtropospheric height field, several characteristics of the Ac-EW jets suggest that boundary layer processes are stronger than for Ac-SWNE jets. Specifically, AC-EW jets were only observed in the early morning hours (1200 UTC), had a very shallow elevation (median height 942 mb), and displayed fairly strong clustering of the jet cores about a median location of 36°N. On the other hand, Ac-SWNE jets were observed at higher elevations and lacked a clear diurnal preference for the morning hours. Furthermore, their jet cores displayed more spatial scattering about a median latitude that is farther north (38°N).

The composite fields for the Ac-EW and Ac-SWNE jets both confirm and contradict previous findings. Similar to the findings of early studies (e.g., Wexler 1961;

Bonner 1968), Ac-SWNE jets are embedded in an anticyclonically curved airstream within the return flow of a strong Bermuda high, although earlier studies did not point out that the broader-scale composite pressure pattern resembles a col with two additional, but weaker, circulation features located immediately north of the wind maximum. The composite wind fields for the Ac-SWNE jets suggest that the geostrophic contribution to the wind speed is more important than the ageostrophic contribution. This finding diverges from the classic conception that ageostrophic influences are larger than pressure gradient forcing for boundary layer low-level wind maxima. On the other hand, and in line with previous findings, the ageostrophic component is larger than the geostrophic component for Ac-EW jets. Like Ac-SWNE jets, the composite sea level pressure pattern for Ac-EW jets also resembles a col. However, in this case the strongest system is the anticyclone located to the northwest of the jet core rather than the anticyclone to the southeast. In other words, the Bermuda high is much weaker for Ac-EW jets than for Ac-SWNE jets. Another important finding of this study is that the location of the jet cores for the supergeostrophic Ac-EW jet events cannot be attributed to a local maximum in either the geostrophic or the ageostrophic wind. The jet core is rather the result of a combination of relatively large geostrophic wind vectors to the southwest and southeast of the jet core and large ageostrophic vectors to the west of the jet core.

b. Low-level wind maxima in active environments

One important finding of this study is the remarkable variation in the airflow configuration of low-level wind maxima that occur in an active setting. Some of the variation possibly results from different stages in the evolution of low-level wind maxima. Several authors have shown that the orientation of airstreams and low-level wind maxima varies over the life cycle of a midlatitude cyclone (Djuric and Damiani 1980; Trier and Parsons 1993; Bierly and Winkler 2001). This cannot completely explain the observed configuration types, however, as the synoptic and subsynoptic-scale environment differs substantially between some of the types.

One aspect of the large-scale environment that differs among types is the sea-level pressure pattern. While the jet core for all configuration types is located along the western edge of a pressure gradient between a high pressure cell over the eastern or southeastern United States and a trough of low pressure over the central and western United States, the location, size, and strength of these pressure systems differ. The relative location of the anticyclone over the eastern United States compared with the jet core is key in determining the orientation of the wind maximum. For anticyclonically curved flow, the high pressure cell is located south of the latitude of the jet core, compared with a more northern location of the high pressure cell for cyclonically curved jets. When additional pressure cells are located downstream of the wind maximum, bifurcating flow frequently results.

The jet types with the highest wind speeds appear to result from both a favorable synoptic environment and favorable boundary layer conditions. This finding supports earlier studies by Uccellini (1980) and Mitchell et al. (1995). The Kc-SWNE jets, for example, show evidence of both synoptic and boundary layer forcing. Synoptic-scale influences can be inferred from the midtropospheric trough and the superposition of the right entrance quadrant of an upper-level jet streak over the low-level wind maximum. Indications of boundary layer influences are the temporal preference for the morning hours, shallow heights, and a clustering of the jet cores about a more southerly median latitude of 37°N. Also, the geostrophic and ageostrophic wind fields are of similar magnitude for Kc-SWNE jets, although one impact of the ageostrophic forcing is to displace the jet core to the south of the strongest pressure gradient.

Other jet types with approximately equal contributions of the ageostrophic and geostrophic components of the actual wind are the Cc, LCc, and LBKc-SWNE jets. All three types are located due east of a low pressure system. However, only for the Cc jets do the ageostrophic vectors coincide with a region of large 12-h pressure falls, suggesting an isallobaric contribution to the ageostrophic wind field. For the LCc and LBKc-SWNE jets, the ageostrophic vectors are rotated to the west of the actual wind, even though the wind maxima themselves are directed toward an area of pressure falls. This complex pattern suggests that other factors in addition to isallobaric forcing are important.

The relationship between the Cc, LCc, and LBKc-SWNE jet types to previously identified airstreams within cyclones is complex. Although wind maxima have been observed embedded within the warm conveyor belt of midlatitude cyclones (Carlson 1980; Carr and Millard 1985), the configuration of the Cc, LCc, and LBKc-SWNE jets differs from the typical anticyclonic curvature of the warm conveyor belt (Carlson 1980). It should be kept in mind, however, that these jet maxima are often complex (see Table 2 from Part I) and may have multiple airstreams. As shown in Part I, the airflow at the upper levels is often more anticyclonic in character. An alternative explanation is that the lower levels of the Cc, LCc, and LBKc-SWNE jets are part of the cyclonically turning moist airstream that Bierly and Winkler (2001) identified as an important feature of Colorado cyclones or the fanlike trajectories identified by Mass and Schultz (1993) for a simulated wintertime cyclone, whereas the upper levels are part of the anticyclonic-turning warm conveyor belt.

For the remaining six types of low-level wind maxima in an active environment (i.e., Bd-SWNE, Bd-NWSE, LAc-SWNE, L2A, LB, and LKc-SWNE jets), the geostrophic wind component is greater than the ageostrophic; in other words, pressure gradient forcing dominates.

However, the locations of the strongest geostrophic wind vectors and the jet core do not coincide. The actual wind maximum is displaced to the west or southwest of the strongest pressure gradient. This indicates that knowledge of the ageostrophic wind is essential in understanding the location of the jet core. An interesting observation is that these jet types are either equally frequent during night and day and/or occur at relatively high elevations. In contrast, jets with strong ageostrophic components primarily occur at night and have average altitudes close to the earth's surface.

6. Summary

Southerly low-level wind maxima in the Great Plains that occurred in the warm seasons (Apr–Sep) of 1991–92 were studied to better define the climatological characteristics of these events. The focus of Part I was to identify the physical characteristics of low-level wind maxima, particularly the spatial configuration of the airflow patterns. Here, in Part II, the large-scale environment in which wind maxima with different airflow configurations occur was investigated. The major findings of Part II can be summarized as follows:

- Most Great Plains low-level wind maxima are synoptically driven, or in other words, form in an active environment. Only 2 of the 12 types, comprising 17% of the total number of jet events for the study period, were found to occur with a midtropospheric ridge (i.e., a quiescent environment).
- Jet types that form in a quiescent environment appear to have fairly simple, anticyclonically curved airflow, whereas those that form in an active environment display more complex airflow. Also, jet types that form in quiescent environments have limited latitudinal extent.
- Jet types that occur in a quiescent environment are associated with a col in the sea level pressure pattern. On the other hand, the sea level pressure pattern for jet types that form in an active environment consists of a high pressure cell to the east of the jet core and a trough of low pressure to the west of the jet core. The configuration of the wind maximum is related to the relative location of the anticyclone. For anticyclonically curved flow the high pressure cell is located south of the latitude of the jet core, whereas for cyclonically curved jets the high pressure cell is located at the same latitude or to the north of the jet core. Bifurcating flow results when additional pressure cells are located downstream of the wind maximum.
- The relative magnitude of the geostrophic wind component to the ageostrophic wind component varies with jet type. In general, jet types with relatively strong ageostrophic components were most frequently observed at night and/or at comparatively shallow heights. These results suggest that the relative influence of pressure gradient forcing versus boundary-layer forcing varies with jet type, regardless of whether the large-scale environment is quiescent or active.
- The location of jet cores, regardless of airflow configuration type, is usually displaced from the area of the strongest pressure gradient, and is determined by a combination of pressure gradient and ageostrophic forcing.
- For almost all jet types, an area of large ageostrophic wind vectors is located to the northwest of the jet core. In general, these vectors point toward the confluence boundary along the left flank of the low-level wind maximum, and are speculated to be part of a transverse circulation around the confluence/frontal zone. Also, a second area of strong ageostrophic wind vectors is found southwest of the jet core in an area with a marked moisture gradient (i.e., a dryline). Another characteristic of almost all jet types is a veering (i.e., anticyclonic rotation) of the ageostrophic wind vectors with latitude upstream of the jet core.
- Finally, warm season low-level wind maxima in the Great Plains are usually associated with the right entrance region of an anticyclonically curved upper-level jet stream and an associated region of upper-level divergence.

The results of this climatological study will hopefully contribute to an improved understanding of the variability of low-level wind maxima, provide valuable guidance when forecasting convection in association of low-level wind maxima, and help in the understanding and integration of the many previous case studies of low-level wind maxima.

Acknowledgments. The author would like to thank Julie Winkler for her advice in developing this project and helpful comments in preparing this manuscript. Jim Brown's assistance with the data processing is greatly appreciated. The thoughtful and constructive comments provided by three anonymous reviewers helped improve the manuscript and are gratefully acknowledged. Software for the analyses and displays presented in this paper was acquired through the Unidata Program, which is sponsored by the National Science Foundation and overseen by the University Corporation for Atmospheric Research. The analysis/display software (GEMPAK) was provided to Unidata by NASA Goddard and the National Weather Service.

REFERENCES

Achtor, T. H., and L. H. Horn, 1986: Spring season Colorado cyclones. Part I: Use of composites to relate upper and lower tropospheric wind fields. *J. Climate Appl. Meteor.*, **25,** 732–743.

Beebe, R. G., and F. C. Bates, 1955: A mechanism for assisting in the release of convective instability. *Mon. Wea. Rev.*, **83,** 1–10.

Bierly, G. D., and J. A. Winkler, 2001: A climatological analysis of airstreams within cold season cyclones originating in the Colorado cyclogenesis region of the United States. *Wea. Forecasting*, **16,** 57–80.

Blackadar, A. K., 1957: Boundary layer wind maxima and their sig-

nificance for the growth of nocturnal inversions. *Bull. Amer. Meteor. Soc.,* **38,** 283–290.
Bonner, W. D., 1968: Climatology of the low level jet. *Mon. Wea. Rev.,* **96,** 833–850.
——, and J. Paegle, 1970: Diurnal variations in boundary layer winds over the south-central United States in summer. *Mon. Wea. Rev.,* **98,** 735–744.
——, S. Esbensen, and R. Greenberg, 1968: Kinematics of the low-level jet. *J. Appl. Meteor.,* **7,** 339–347.
Browning, K. A., and C. W. Pardoe, 1973: Structure of low-level jet streams ahead of mid-latitude cold fronts. *Quart. J. Roy. Meteor. Soc.,* **99,** 619–638.
Buajitti, K., and A. K. Blackadar, 1957: Theoretical studies of diurnal wind-structure variations in the planetary boundary layer. *Quart. J. Roy. Meteor. Soc.,* **84,** 486–500.
Carlson, T. N., 1980: Airflow through midlatitude cyclones and the comma cloud pattern. *Mon. Wea. Rev.,* **108,** 1498–1509.
Carr, F. H., and J. P. Millard, 1985: A composite study of comma clouds and their association with severe weather over the Great Plains. *Mon. Wea. Rev.,* **113,** 370–387.
Chen, T.-C., and J. A. Kpaeyeh, 1993: The synoptic-scale environment associated with the low-level jet of the Great Plains. *Mon. Wea. Rev.,* **121,** 416–420.
Chen, Y.-L., X. A. Chen, and Y.-X. Zhang, 1994: A diagnostic study of the low-level jet during TAMEX IOP 5. *Mon. Wea. Rev.,* **122,** 2257–2284.
Djuric, D., 1981: A numerical model of the formation and evolution of a low-level jet. *Mon. Wea. Rev.,* **109,** 384–390.
——, and M. S. Damiani Jr., 1980: On the formation of the low-level jet over Texas. *Mon. Wea. Rev.,* **108,** 1854–1865.
——, and D. S. Ladwig, 1983: Southerly low-level jet in the winter cyclones of the southwestern Great Plains. *Mon. Wea. Rev.,* **111,** 2275–2281.
Fast, J. D., and M. D. McCorcle, 1990: A two-dimensional numerical sensitivity study of the Great Plains low-level jet. *Mon. Wea. Rev.,* **118,** 151–163.
Hering, W. S., and T. R. Borden Jr., 1962: Diurnal variations in the summer wind field over the central United States. *J. Atmos. Sci.,* **19,** 81–86.
Hoecker, W. H., 1963: Three southerly low-level jet systems delineated by the Weather Bureau special PIBAL network of 1961. *Mon. Wea. Rev.,* **91,** 573–582.
——, 1965: Comparative physical behavior of southerly boundary-layer wind jets. *Mon. Wea. Rev.,* **93,** 133–144.
Hovanec, R. D., and L. H. Horn, 1975: Static stability and the 300 mb isotach field in the Colorado cyclogenetic area. *Mon. Wea. Rev.,* **103,** 628–638.
Hoxit, L. R., 1975: Diurnal variations in planetary boundary-layer winds over land. *Bound.-Layer Meteor.,* **8,** 21–38.
Igau, R. C., and J. W. Nielsen-Gammon, 1998: Low-level jet development during a numerically simulated return flow event. *Mon. Wea. Rev.,* **126,** 2972–2990.
Izumi, Y., 1964: The evolution of temperature and velocity profiles during breakdown of a nocturnal inversion and a low-level jet. *J. Appl. Meteor.,* **3,** 70–82.
Koch, S. E., M. des Jardins, and P. J. Kocin, 1983: An interactive Barnes objective map analysis scheme to use with satellite and conventional data. *J. Climate Appl. Meteor.,* **22,** 1487–1503.
Kotroni, V., Y. Lemaitre, and M. Petitdidier, 1994: Dynamics of a low-level jet observed during the Fronts 87 experiment. *Quart. J. Roy. Meteor. Soc.,* **120,** 277–303.
Mass, C. F., and D. M. Schultz, 1993: The structure and evolution of a simulated mid-latitude cyclone over land. *Mon. Wea. Rev.,* **121,** 889–917.
McNulty, R. P., 1978: On upper tropospheric kinematics and severe weather occurrence. *Mon. Wea. Rev.,* **106,** 662–672.
Mitchell, M. J., R. W. Arritt, and K. Labas, 1995: A climatology of the warm season Great Plains low-level jet using wind profiler observations. *Wea. Forecasting,* **10,** 576–591.
Paegle, J., and G. E. Rasch, 1973: Three-dimensional characteristics of diurnally varying boundary-layer flows. *Mon. Wea. Rev.,* **101,** 746–756.
Parish, T. R., A. R. Rodi, and R. D. Clark, 1988: A case study of the summertime Great Plains low level jet. *Mon. Wea. Rev.,* **116,** 94–105.
Sechrist, F. S., and T. M. Whittaker, 1979: Evidence of jet streak vertical circulations. *Mon. Wea. Rev.,* **107,** 1014–1021.
Sjostedt, D. W., J. T. Sigmon, and S. J. Colucci, 1990: The Carolina nocturnal low-level jet: Synoptic climatology and a case study. *Wea. Forecasting,* **5,** 404–415.
Stensrud, D. J., 1996: Importance of low-level jets to climate: A review. *J. Climate,* **9,** 1698–1711.
Trier, S. B., and D. B. Parsons, 1993: Evolution of environmental conditions preceding the development of a nocturnal mesoscale convective complex. *Mon. Wea. Rev.,* **121,** 1078–1098.
Uccellini, L. W., 1980: On the role of upper tropospheric jet streaks and leeside cyclogenesis in the development of low-level jets in the Great Plains. *Mon. Wea. Rev.,* **108,** 1689–1696.
——, 1990: The relationship between jet streaks and severe convective storm systems. Preprints, *16th Conf. on Severe Local Storms.* Kananaskis Park, AB, Canada, Amer. Meteor. Soc., 121–130.
——, and D. R. Johnson, 1979: The coupling of upper and lower tropospheric jet streaks and implications for the development of severe convective storms. *Mon. Wea. Rev.,* **107,** 682–703.
Walters, C. K., and J. A. Winkler, 2001: Airflow configurations of warm season southerly low-level wind maxima in the Great Plains. Part I: Spatial and temporal characteristics and relationship to convection. *Wea. Forecasting,* **16,** 513–530.
Wexler, H., 1961: A boundary layer interpretation of the low-level jet. *Tellus,* **13,** 368–378.
Whittaker, L. M., and L. H. Horn, 1981: Geographical and seasonal distribution of North American cyclogenesis, 1958–1977. *Mon. Wea. Rev.,* **109,** 2312–2322.
Zeman, O., 1979: Parameterization of the dynamics of stable boundary layers and nocturnal jets. *J. Atmos. Sci.,* **36,** 792–804.
Ziegler, C. L., and C. E. Hane, 1993: An observational study of the dryline. *Mon. Wea. Rev.,* **121,** 1134–1151.